

Review

# Nanostructure of Superlubricating Tribofilm Based on Friction-Induced a-C:H Films under Various Working Conditions: A Review of Solid Lubrication

Xuan Yin <sup>1,\*</sup>, Linyuan Mu <sup>1</sup>, Zihang Jia <sup>1</sup>, Haosheng Pang <sup>2,\*</sup>, Chunpeng Chai <sup>3,\*</sup>, Huan Liu <sup>4</sup>, Chang Liang <sup>1</sup>, Bing Zhang <sup>1</sup> and Dameng Liu <sup>4</sup>

<sup>1</sup> College of Mechanical and Electrical Engineering, Beijing University of Chemical Technology, Beijing 100029, China; 2021030059@buct.edu.cn (L.M.); 2021030475@buct.edu.cn (Z.J.); liangchang@mail.buct.edu.cn (C.L.); zhangbing@mail.buct.edu.cn (B.Z.)

<sup>2</sup> Chinese Aeronautical Establishment, Beijing 100012, China

<sup>3</sup> School of Materials Science and Engineering, Beijing Institute of Technology, Beijing 100081, China

<sup>4</sup> State Key Laboratory of Tribology in Advanced Equipment, Department of Mechanical Engineering, Tsinghua University, Beijing 100084, China; liuhuanskl@163.com (H.L.); ldm@tsinghua.edu.cn (D.L.)

\* Correspondence: yinxuan@buct.edu.cn (X.Y.); panghs.2020@tsinghua.org.cn (H.P.); chaicp@bit.edu.cn (C.C.)

**Abstract:** Diamond-like carbon (DLC) film has gained widespread popularity as a versatile and important solid lubricant material in the field of tribology. Among various types of DLC films, hydrogen-rich DLC (a-C:H) film as a high-performance material has greatly enhanced anti-friction and anti-wear. However, despite its remarkable capabilities, the surface chemical properties and tribological performance of a-C:H film are significantly influenced by the surrounding environment, in special atmospheric conditions. Its super-slip mechanism involves the participation of hydrogen atoms, which can weaken the normal electron number of the outermost layer of a-C:H film. What is more, it is essential to investigate tribofilms in a vacuum or inert gas environment to ascertain the appropriate tribological properties of a-C:H film, which helps in mitigating oxidation effects. When non-doped DLC films are subjected to friction in a dry nitrogen or argon environment, they create sp<sup>3</sup>-C-rich transfer films on the contact surface, resulting in macroscopic super-slip effects. This paper aims to introduce and discuss the diverse nanostructures of in situ tribofilms in a-C:H film, focusing on the working environment, and explore the prospective application directions of a-C:H film.

**Keywords:** diamond-like carbon film; tribofilm; two-dimensional materials; lubrication mechanism



**Citation:** Yin, X.; Mu, L.; Jia, Z.; Pang, H.; Chai, C.; Liu, H.; Liang, C.; Zhang, B.; Liu, D. Nanostructure of Superlubricating Tribofilm Based on Friction-Induced a-C:H Films under Various Working Conditions: A Review of Solid Lubrication. *Lubricants* **2024**, *12*, 40. <https://doi.org/10.3390/lubricants12020040>

Received: 25 December 2023

Revised: 22 January 2024

Accepted: 29 January 2024

Published: 31 January 2024



**Copyright:** © 2024 by the authors. Licensee MDPI, Basel, Switzerland. This article is an open access article distributed under the terms and conditions of the Creative Commons Attribution (CC BY) license (<https://creativecommons.org/licenses/by/4.0/>).

## 1. Introduction

Diamond-like carbon (DLC) is a synthetic material that has garnered significant attention due to its unique properties, making it an excellent coating material for various mechanical devices. As a widely engineered and industrial application, DLC film has already been utilized in engines and bearings resulting in a friction coefficient lower than 0.01 (a superlubricity state [1,2]). Superlubricity helps reduce friction and wear, thereby extending the life of materials. The superlubricity of DLC is due to the formation of a highly ordered tribofilm with a thickness of only a few nanometers. This highly ordered structure reduces the friction between surfaces, resulting in superlubricity. The growing focus on superlubric DLC has caught the attention of many. Besides its excellent tribological performance, carbon thin film also possesses low surface energy, which has been explored in diversified superlubricity pathways. Super-low friction and wear are common characteristics of DLC films, which exhibit significant tribological behaviors and negligible energy consumption during rubbing. As a representative of amorphous carbon (a-C) films in relevant tribological fields [3–6], DLC film has bonding structures and properties resembling both diamond (sp<sup>3</sup>-C phase) and graphite (sp<sup>2</sup>-C phase), as shown in Figure 1.

Among various types of DLC films, hydrogen-rich DLC (a-C:H) films have been successfully designed to achieve ultra-low (friction coefficient  $< 0.1$ ) or even super-low (friction coefficient  $< 0.01$ ) friction in dry inert atmospheres like dry nitrogen atmospheres. This is mainly attributed to the buildup of a nanostructured graphitic tribofilm (a thin film that forms on the surface of an induced-friction transfer substance, reducing its abrasion) and the associated surface passivation from  $-H$  or  $-OH$  free groups along the sliding interface [7–9]. This kind of induced-friction transfer substance is called a tribofilm, which does not have any hardness and cannot be tested independently. Essentially, a tribofilm is a substance generated through physical action or a chemical reaction induced by shear force during the friction process. The tribological performances are obtained by characterizing the contact structure and friction coefficient of the friction pair that carries the transfer film. However, when friction occurs in the atmosphere, the structure of the a-C:H film surface is easily destroyed due to O and moisture-induced strong tribochemical reactions [10–12], leading to the failed protection of materials or key mechanical moving parts. The tribofilm generated by the DLC coating possesses a distinct nanoscopic structure, smaller than a micrometer. The superlubricating property of DLC can be ascribed to the aforementioned nanoscopic structure of the tribofilm. The tribofilm generated by DLC exhibits a highly organized arrangement and is only a few nanometers thick. Therefore, it is crucial to comprehensively investigate the nanostructures of in situ tribofilms on the contacts for broadened environments.

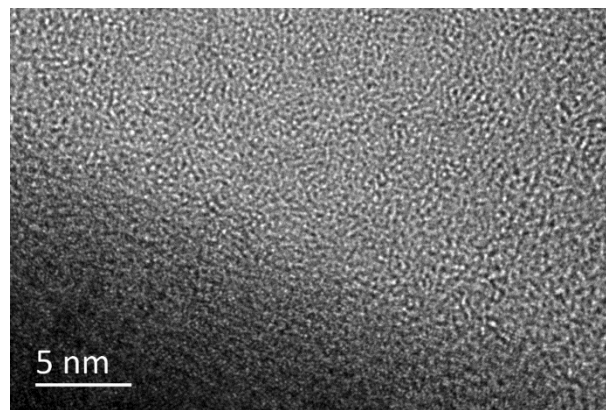


**Figure 1.** HRTEM images showing the atomic microstructures of DLC film.

In the past decade, low-dimensional (2D) materials and zero-dimensional (0D) materials have been extensively studied as efficient alternatives for surface modification, to exploit novel superlubricity systems. Graphene, 2D titanium carbide ( $Ti_3C_2$ , one type of MXenes), graphene quantum dots (GQDs), and nanodiamonds, owing to their special atomic-scale structure, are gradually being utilized in fundamental applied research [13–17]. In general, the combination of DLC films and low-dimensional materials has become the core of modified solid lubrication films. The major characterizations of in situ tribofilm nanostructures are high-resolution transmission electron microscopy (HRTEM), the focused ion beam–scanning electron microscopy dual-beam system (SEM-FIB), and dual-aberration-corrected scanning transmission electron microscopy and electron energy-loss microscopy (STEM-EELS) [15,18–21]. These characterization methods have already been utilized in the interfacial structure and surface morphology of materials for basic research and mechanical engineering applications. In a few research groups aspiring to investigate the nanostructures of in situ tribofilms, our group has carried out a large amount of work based on the structures and characterizations of macro-lubrication. Due to the drawbacks of DLC films, their surface properties need to be modified or matched with proper tribocouples to meet the increasingly stringent requirements of superlubricity in complicated working conditions. In previous experiments [15,16,22], we found that nanocoating, which is utilized as a highly effective solid lubricant, accelerated the formation of the tribofilm

as a protective surface layer, especially in a dry nitrogen atmosphere. In addition, the selection of friction counterparts has a significant impact on tribological performances and in situ tribofilm structures in mechanical engineering [19,23–28]. Mechanical performances such as hardness and elastic modulus exert the most pivotal influence on the tribological behaviors of the tribo-couples. Commonly, among the counterpart materials, steel [29,30] and ceramic [26,31] are the most frequently used tribo-couples through intensive adhesive or abrasive interactions between sliding surfaces. DLC-based steel or silicon nitride sliding against the same type of film material substrate (namely a self-mated system) has the superiority to establish the superlubricity state (friction coefficient namely  $\mu < 0.01$ ). During the sliding process, the contact surfaces of the counterfaces are usually covered by forming an in situ tribofilm to reduce friction and wear [9]. The nanostructures of in situ tribofilms are governed by tribophysics and tribochemistry on the interfacial contacts. Weak interactions along the sliding interface are accordingly realized by low-shear-strength lubrication phases such as the  $sp^2$ -C phase or the highly passivated contact surfaces induced by van der Waals forces such as the  $sp^3$ -C phase [6].

It is crucial to choose the appropriate friction counterparts to optimize the overall performance and efficiency of mechanical systems. The selection process involves considering various factors such as material compatibility, load capacity, and environmental conditions [23,25]. The design of tribo-couples also plays a crucial role in reducing wear and increasing the lifespan of moving components. The geometry, surface roughness, and lubrication strategies are carefully evaluated and implemented to minimize friction and enhance tribological performances. For instance, steels [29,30] and ceramics [31,32] are the most commonly used substrates among the counterpart materials. Generally, the mechanical properties, such as hardness and elastic modulus, have the most significant influence on the tribological behaviors of tribo-couples. Additionally, friction and wear are also greatly affected by the surface morphologies and bonding chemistry of the counterparts [24,33]. To improve the sliding accommodation to the working conditions, the surfaces of mechanical components are typically coated with a layer of solid film or lubricated with various lubricants [34]. With breakthroughs in technological methods and algorithm innovations, there have been significant advancements in the study of DLC friction behavior, specifically the microstructure of transfer films. These approaches have provided valuable insights into the interactions, conformational changes, and dynamic processes between molecules within transfer films, shedding light on their formation mechanisms, stability, and functionality [35,36]. Simulating the interactions between molecules in transfer films allows for the investigation of changes in parameters such as binding forces, bond lengths, and angles, thereby exploring the mechanisms behind transfer film formation. Furthermore, molecular dynamics (MD) can simulate the movement of molecules within transfer films, including torsion, rotation, and displacement, providing insights into conformational changes and dynamic processes.

To date, there has been a lack of comprehensive summaries regarding the nanostructures of in situ tribofilms that induce superlubricity for DLC films. Therefore, this paper aims to introduce and discuss the diverse nanostructures of in situ tribofilms that induce superlubricity for DLC films. The influencing factors of superlubricating tribofilm nanostructures are also considered, with a focus on the working environment atmosphere (such as atmospheric, dry inert, harsh, and humid environments), which is supplemented with computational simulation techniques. Furthermore, the lubrication mechanisms of obtained tribofilms based on various working conditions are summarized at the end of the paper. This paper provides perspectives on the nanostructures of in situ tribofilms that induce superlubricity, particularly in the field of surface engineering. Our goal is to establish a system that provides useful guidance for understanding and analyzing the nanostructures of in situ tribofilms for DLC films and solid lubrication films. Meanwhile, we hope that interested researchers will offer valuable suggestions for characterizations and the analysis of nanostructures of in situ tribofilms.

## 2. Atmospheric Environment

### 2.1. Nanostructure of Transfer Film

Atmospheric conditions at room temperature are commonly used operating environments for aircraft, cars, high-speed trains, ships, and other vehicles. In such environments, it is crucial to investigate the structure of the super-slippery surface of a-C to guide the improvement of surface lubrication for large critical motion mechanisms operating in atmospheric conditions at room temperature. In the atmospheric environment, the lowest  $\mu$  of hydrogen-free DLC is 0.016, as shown in Table 1. The reason for the low  $\mu$  is that under strong shear, there is unstable  $sp^3$ -C bond break and bond length and direction change, causing adjacent atoms to rearrange carbon bonds along the shear direction to reduce lattice strain energy. Ultimately, transfer materials containing discontinuous graphite nanocrystalline (cluster clusters) are formed on the contact surface, and much complete amorphous carbon is generated along the direction of maximum shear stress [37]. After hydrogen doping, the  $\mu$  of DLC can be further reduced to 0.005, resulting in a super-slippery state, as shown in Figure 2. The mechanism behind this effect is that the participation of hydrogen weakens the normal electron number of the outermost layer of the a-C:H film's electric dipole. Due to the lower van der Waals force, the terminal hydrogen bonds randomly distribute and passivate the outermost electrons, further weakening the induced electric dipole moment and obtaining a lower polarization rate. Finally, a transfer film composed of curved multilayer graphene strips or onion-shaped carbon nanoparticles is formed in situ on the sliding contact surface, effectively reducing the  $\mu$  and wear rate [27,38,39]. When other elements, such as Cr, are doped into amorphous carbon film, excluding hydrogen, it is found that the  $\mu$  increases. This is because Cr is a hard metallic element that enhances the hardness of the contact surface, resulting in the structure of the transfer film being mainly composed of  $sp^2$ -C and Cr [40]. Other carbon-based amorphous films, such as onion-like carbon (OLC) and hydrogenated fullerene-like carbon (FL-C:H), also exhibit extremely low  $\mu$ . The  $\mu$  of OLC can reach 0.01, and the wear rate is also extremely low at  $6.41 \times 10^{-18} \text{ mm}^3/\text{Nm}$ . Onion-like carbon can slide as a nanoscale "rolling bearing" during the friction process, providing an amorphous contact interface between the friction contact surface and the OLC film. In situ this generates an interface transfer film combining onion-like carbon and graphitized carbon, thereby achieving ultra-low friction-wear, and greatly reducing energy loss [41]. The  $\mu$  of FL-C:H film is also less than 0.02, and a transfer film is generated in situ on the friction-sliding surface induced by friction. The composition of the transfer film is composed of pentagonal and heptagonal carbon rings and hexagonal graphene rings caused by the thermal and strain effects of repeated friction. These polygonal ring-shaped carbon structures form a stable fullerene-like structure, thereby achieving ultra-low friction and wear of FL-C:H in the atmospheric environment.

**Table 1.** Tribological data of DLC film under different working conditions.

Environment	Sample	Stable $\mu$	Wear Rate ( $\text{mm}^3/\text{Nm}$ )	Reference
Atmosphere	a-C	0.016		[37]
	a-C:H	0.005		[27,38,39]
	a-C:Cr			[40]
	OLC	0.01	$6.41 \times 10^{-18}$	[41]
	FL-C:H	<0.02		[41]
Dry inert	a-C:H	0.001–0.003	$4.6 \times 10^{-10}$	[42]
	GLC	0.005		[43]
	FLC	0.009		[43]
	B <sub>4</sub> C/a-C	0.035		[44]
	TaC/a-C	0.002	$8.80 \times 10^{-10}$	[45]
	GQDs/a-C:H	0.01		[15,16]
Combustible gas-H <sub>2</sub> -CH <sub>4</sub>	a-C:H	0.0001		[46,47]
	a-C:H	0.0093	$8.0 \times 10^{-8}$	[48–50]
Ultra-high vacuum	a-C:H	0.003–0.02	$4.6 \times 10^{-10}$	[51,52]
Moisture	GO/a-C:H:Si	0.002		[53]

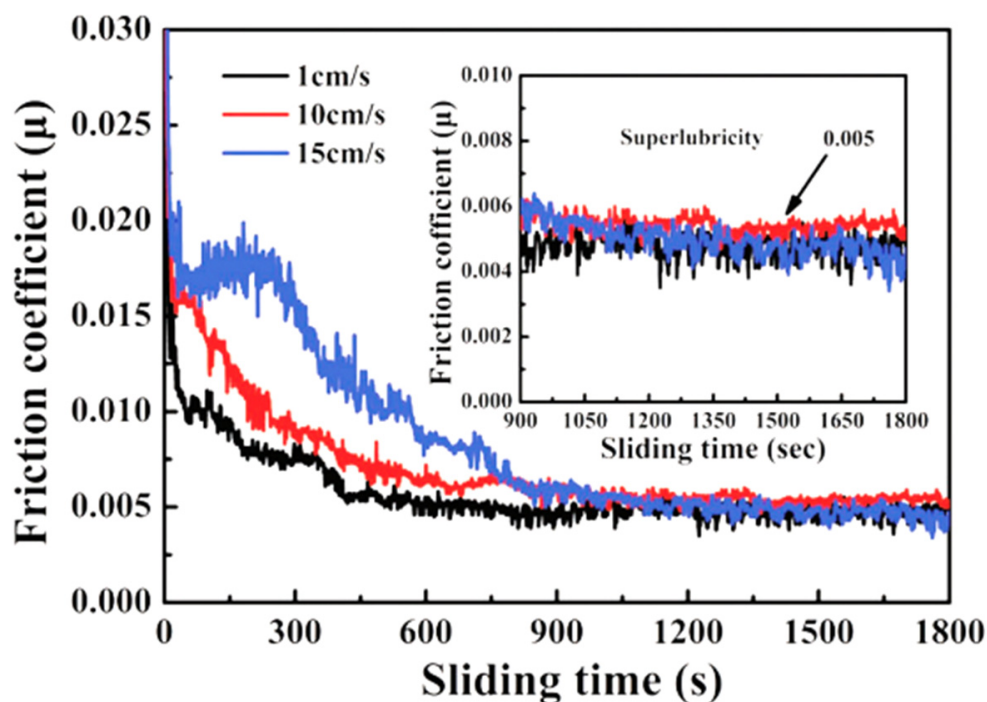


**Figure 2.** Experimental demonstration of the superlubricity regime for a-C:H film under 1, 10, and 15 cm/s linear velocity (air environment, room temperature, 2.89 GPa contact pressure) Rprinted with permission from Ref. [38]. Copyright 2017, WILEY-VCH Verlag GmbH & Co. KGaA, Weinheim.

In addition to regulating the composition ratio of C, H, and F in DLC and the hybrid structure of C, excellent lubrication effects can also be achieved by coating the surface with a coating. By coating graphene or modified MXenes on the polymer-like carbon (PLC) surface, it is found that the  $\mu$  is less than 0.1, and the wear rate is at the level of  $10^{-8}$  mm<sup>3</sup>/Nm. The structure of the transfer film is mainly composed of low molecular weight polyacrylic acid forming a more ordered sp<sup>2</sup>-C phase. Additionally, the surface-active groups of MXenes participate in the formation of multilayer lubricating transfer films [16,54].

## 2.2. Effects on Surface Structure

Through the study of the structure of transfer films, it can be observed that the air environment has a significant impact on the termination groups of the DLC surface, especially a-C:H film. Firstly, oxygen in the air reacts with the hydrogen atoms on the surface of a-C:H film, resulting in the formation of oxide surfaces. This will change the physicochemical characteristics of the a-C:H surface, such as the surface energy and friction coefficient. Additionally, oxide surfaces can reduce the hydrophobicity of a-C:H, reducing its lubricating performances [55,56]. Therefore, in applications where high lubrication requirements or key friction performance are needed, oxygen in the air may cause a decrease in the surface performances of a-C:H film. Secondly, in addition to oxygen, there may be other pollutants in the air, such as moisture and organic compounds [57,58]. These pollutants can interact with the surface of a-C:H film through adsorption or reaction. For example, moisture can cause hydrolysis reactions on the surface of a-C:H film, leading to the detachment of hydrogen atoms from the surface and a decrease in the hydrogen content of the DLC surface [59–61]. This will affect the hardness and conductivity of DLC films. For instance, organic pollutants may form adsorption layers on the surface of a-C:H film, affecting its optical transparency and optical performance [62,63]. To address these issues, measures can be taken to reduce the impact of the air environment on the surface terminal groups of a-C:H film. For example, special surface treatment methods, such as surface

modification or coating, can be used to protect the surface terminal groups of a-C:H film and maintain its effective lubricating properties when subjected to friction in the air [64].

### 3. Dry Inert Environment

#### 3.1. Nanostructure of Transfer Film

The room temperature atmospheric environment is currently the most variable service condition environment, including unstable humidity, temperature, and oxygen content. Therefore, by controlling the variables and singling out the service environment, studying the ultra-smooth transfer film structure and lubrication mechanism of amorphous carbon films is beneficial. Among the commonly used methods for controlling service conditions, dry inert environments (such as dry nitrogen and dry argon) are the easiest to implement and operate in the laboratory. The advantage of dry inert gas environments is that they do not react with the upper and lower friction pairs. Their surface coatings remain intact during the friction process, thereby they do not affect the composition of the ultra-smooth transfer film structure.

Several studies by researchers [1,65,66] have found that under dry nitrogen conditions, silicon wafers coated with high-hydrogen DLC (namely 40at.%H-DLC, which is made from 25% methane and 75% hydrogen) films have extremely low  $\mu$ . During the running-in period, the  $\mu$  is 0.15 [67]. During the stable period, the  $\mu$  is 0.001~0.003, and the wear rate is  $4.6 \times 10^{-10} \text{ mm}^3/\text{Nm}$ , as shown in Table 1. The transfer film structure on the surface is mainly composed of amorphous carbon layers. The most directly contacted surface contains a large amount of released hydrogen elements and hydrogenated  $\text{sp}^3\text{-C}$ , which passivate the surface chemically and increase the local density, as shown in Figure 3 [42]. This passivated surface cannot form strong chemical bonds and covalent  $\sigma$  bonds (which can lead to high adhesion/friction) on the sliding interface. The variation results in the enhanced hydrophobicity of the film and reduced possibility of frictional adhesion by reducing the number of carbon dangling bonds, thus achieving ultra-low friction and wear. The friction-induced hydrogenated amorphous carbon layer is crucial to the wear of diamond films. In addition to hydrogenated DLC, graphite-like carbon (GLC) and fullerene-like carbon (FLC) DLC also exhibit ultra-smooth effects. Wang's study [43] found that steel balls and plates coated with GLC or FLC on the surface (i.e., self-mated friction pairs) have extremely low  $\mu$  during wear. The self-mated GLC has a  $\mu$  of 0.005 and forms some ordered graphene layer structures on the sliding interface. These layered structures are formed by GLC through adaptive sliding-direction hybridization and rearrangement along the sliding direction, resulting in a larger and more ordered graphene structure in the transfer film on the surface. The self-mated FLC has a slightly higher  $\mu$  of 0.009. The reason for this is that the spherical nanoparticles with a graphite shell formed on the sliding interface of FLC reduce the contact area. FLC forms spherical nanoparticles with a graphite shell through hybridization and rearrangement from the surface to the center of the particles but partially resists the rearrangement of its graphene layer. Compared with GLC, FLC exhibits a lower degree of hybridization under low and high loads and can only achieve ultra-low friction at higher loads ( $>0.77 \text{ GPa}$ ). Different initial structures of  $\text{sp}^2\text{-C}$  films are transformed into different friction products through different hybridization pathways and achieve ultra-low friction through different friction reduction pathways such as reducing the contact area or interlayer sliding. In other words, the structural characteristics of  $\text{sp}^2\text{-C}$  films determine the transformation pathway in advance, thus producing a friction reduction mechanism in macroscopic contact.

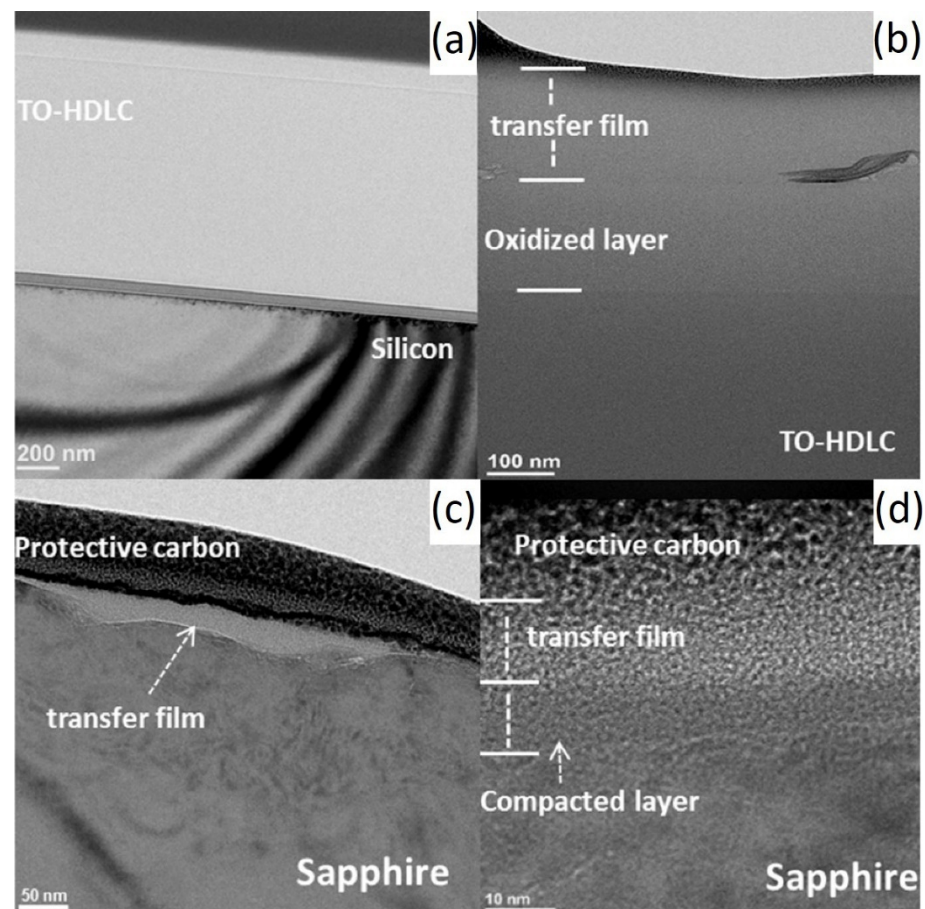


**Figure 3.** HRTEM cross-section images from a-C:H wear track and sapphire hemisphere contact region. (a) Wear track center. (b) Edge of the wear track. (c) Cross-section HRTEM micrograph of the sapphire hemisphere. (d) The transfer film on the sapphire surface. Rprinted with permission from Ref. [42]. Copyright 2017, WILEY-VCH Verlag GmbH & Co. KGaA, Weinheim.

### 3.2. Effects on Surface Structure

The  $\mu$  of amorphous carbon films is between 0.015 and 0.15 [68,69]. In addition to pure amorphous carbon films, doped amorphous carbon films also exhibit excellent tribological properties. Borides are effective graphite catalysts that can accelerate the graphitization process of different carbon materials. The  $\mu$  of  $B_4C/a-C$  films doped with boron carbide ( $B_4C$ ) during wear with steel balls is  $\mu \approx 0.035$ . The reason for this is that under the action of shear force,  $B_4C$  forms a compact and ordered graphite-like carbonaceous tribolayer on the sliding interface of the upper and lower friction pairs, ultimately leading to the low friction and wear of  $B_4C/a-C$  films [44]. In addition, introducing atomically dispersed gold (Au) atoms into the nanocomposite structure of tantalum carbide (TaC)/amorphous carbon (a-C) achieves a  $\mu$  of 0.002 and a wear rate of  $8.80 \times 10^{-10} \text{ mm}^3/\text{Nm}$  [45]. In the initial stage of running-in, high shear forces strip TaC nanoparticles, causing them to roll and merge into larger TaC nanoparticles to reduce surface energy. Meanwhile, under the assistance of shear forces and nano-Au atoms, a-C is graphitized in situ, generating graphite-like carbon (GLC) flakes that wrap TaC particles in the shear layer to form TaC/GLC nanocoils. Finally, a multicontact configuration and non-conforming contact are achieved by obtaining a robust macroscopic ultra-smooth state. Recently, low-dimensional materials such as GQDs, MXenes, and graphene have been preliminarily applied in research on surface engineering. These low-dimensional materials have excellent layered nanostructures, which are beneficial for causing interfacial sliding and accelerating effective lubrication during the frictional process. The sliding counterparts contain transfer layers, namely in situ tribofilms, which act as protective shielding to weaken friction and wear. Through

comprehensive analysis of the interfacial structures of in situ tribofilms, it has been found that the in situ tribofilms always contain some  $sp^2$ -C phase such as nanoflakes. For instance, this is distinctly different from the as-formed nanostructured tribofilm on the contact counterfaces. Studies have shown that the contact surface of the upper counterfacing ball was covered by 2D-layered carbon and graphitic lubricants induced via the structural transformation of GQDs during the whole sliding [15,16]. Meanwhile, the tribofilm of the disk wear track was composed of a silica-like  $SiO_x$  boundary layer and a multicomponent mixed layer induced by tribochemistry. Compared to the self-mated DLC system, the structural boundary enriched with  $SiO_x$  compounds was not formed at the bottom region of the tribofilm for the bare steel system; however, the disk wear track was covered by a thicker tribofilm containing plenty of degraded GQDs. This inferred that the formation of a nanostructured sliding interface was the key to realizing superlubricity.

Dry nitrogen gas does not contain oxygen. Hence, the inert atmosphere does not react with the hydrogen atoms of the contact surface, avoiding the formation of oxide surfaces. The inert connection helps maintain the hydrophilicity of a-C:H and reduces the adsorption or reaction of other pollutants, such as organic compounds. This helps maintain the physical and chemical properties of the DLC surface, thereby maintaining its lubricity and wear resistance.

## 4. Harsh Environment

### 4.1. Combustible Gas Environment

#### 4.1.1. Nanostructure of Transfer Film

Combustible gas environments, such as hydrogen and methane, are also complex service environments. The main concern is to ensure the safety of the friction pair, including the moving mechanism, during the movement process, while also ensuring the safety of personnel. From 1960 to 2000, fuel cells developed rapidly as an important tool for hydrogen utilization. The application practice in aerospace, power generation, and transportation fields fully proves the feasibility of hydrogen as a secondary energy source. The upstream link of hydrogen energy is hydrogen production, mainly including industrial by-product hydrogen, fossil fuel hydrogen production, and renewable energy hydrogen production. The midstream link is hydrogen storage, transportation, and refueling, mainly including low-temperature liquid, high-pressure gas, and solid-state hydrogen storage. Refueling stations are important infrastructure for hydrogen refueling. The downstream link is the fuel cell and application link, and the current main application areas are various fuel-cell vehicles. Therefore, achieving the stable and safe operation of the moving mechanism in a hydrogen environment is imperative. DLC, as a stable and inert film, can maintain great physical and chemical stability in hydrogen.

In a hydrogen environment, the  $\mu$  of DLC is extremely low, reaching 0.0001, as shown in Figure 4. Its super-slip transfer film is composed of hydrocarbons generated by the polymerization of hydrogen and ethanol vapor during the friction process [46,47]. By controlling the surface tribochemistry in a hydrogen environment, DLC films can induce the formation of hydrogen-rich transfer materials on the contact surface, achieving a super-slip state. Methane, as a clean energy source, is one of the pillars of global energy. However, damage to moving parts operating in methane can put pressure on social security and economic development. Hydrogen-rich DLC films are believed to protect moving parts operating in natural gas, mainly composed of methane. At a pressure of 10 kPa, the steady-state  $\mu$  is 0.0093, and the wear rate is  $8.0 \times 10^{-8} \text{ mm}^3/\text{mN}$  [48–50], as shown in Table 1. The transfer film is composed of a graphitized structure in the central region of the contact interface. Meanwhile, by dissociating methane molecules into hydrogen and methane groups, and combining them with carbon dangling bonds, the smoothness of the sliding interface is increased. Through the chemical termination and graphitization process of the sliding interface (the re-hybridization process from  $sp^3$ -C to  $sp^2$ -C), the tribofilm induces a weak interaction between the friction interfaces to achieve low friction and wear.



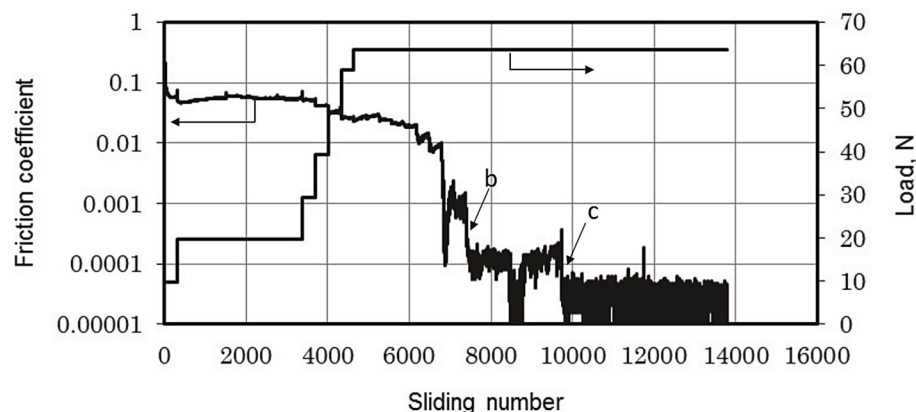


**Figure 4.** Friction coefficient trace. Rprinted with permission from Ref. [46]. Copyright 2017, WILEY-VCH Verlag GmbH & Co. KGaA, Weinheim.

#### 4.1.2. Effects on Surface Structure

In a combustible gas environment, the termination groups on the a-C:H surface may be susceptible to erosion and reaction by gas molecules. For a-C:H film, the bond between hydrogen and carbon atoms is very strong, giving it high chemical stability. However, there may be unique reaction mechanisms in combustible gases that can lead to the decomposition or alteration of the termination groups on the a-C:H surface. The specific reaction mechanisms are as follows:

Firstly, gas molecule adsorption, where molecules in combustible gases can adsorb onto the terminal groups on the a-C:H surface. This adsorption can result in structural changes or the formation of new chemical bonds in the terminal groups. Secondly, gas molecule reaction, where molecules in combustible gases can chemically react with the terminal groups on the film surface [70]. This reaction can lead to the breaking, alteration, or formation of new chemical bonds in the terminal groups. Thirdly, gas molecule erosion, where molecules in combustible gases can physically or chemically erode the a-C:H surface [71]. This erosion can cause damage or detachment of the a-C:H film and even the matrix, thereby affecting its lubricity, wear resistance, and other physical and chemical properties.

### 4.2. Ultra-High Vacuum Environment

#### 4.2.1. Nanostructure of Transfer Film

With the development of vacuum acquisition technology, vacuum applications are increasingly expanding into various aspects of industry and scientific research. Vacuum applications refer to the use of the physical environment of rarefied gases to complete specific tasks. The energy transfer in outer space outside the atmosphere is similar to that in an ultra-high vacuum. Therefore, an ultra-high vacuum can be used for space simulation. Under ultra-high vacuum conditions, the time for the formation of a single molecular layer is long (in hours), which can be used to study surface properties. Before being contaminated by gas, vacuum conditions take advantage of a sufficiently long time for the formation of a contact surface.

Atomic-scale friction behavior mainly depends on chemical reactions and interactions on the friction interface. Friction experiments with DLC in an ultra-high vacuum can reveal interface reactions and atomic-scale wear mechanisms. The results show that the  $\mu$  of a-C:H is  $<0.02$ . Under the action of a frictional force, the hydrogen concentration and methane gas emission in the transfer film structure are high, and this interface emission induces DLC atomic-level chemical wear. With the increase in hydrogen concentration in a-C:H, chemical wear and mechanical wear increase and decrease, respectively. Total wear shows a concave hydrogen concentration dependence, with an optimal hydrogen concentration of about 20% [51,52]. Injecting low-temperature nitrogen into the ultra-high vacuum environment, DLC's  $\mu$  can be further reduced to 0.003, with the wear rate of almost

zero ( $4.6 \times 10^{-10} \text{ mm}^3/\text{Nm}$ ), as shown in Table 1. A graphitized structure was also found in its transfer film structure, and a local friction-induced increase in the content of  $\text{sp}^2\text{-C}$  bonds (Figure 5), thereby achieving ultra-low friction and wear of the hard carbon film. Among a-C:H films against various ceramic-based balls, the significant reason for the failure in superlubricity is attributed to the van der Waals force [72]. The weak interface adhesion between the  $\text{Al}_2\text{O}_3$ /a-C:H interfaces helps to maintain a stable tribofilm on the surface of the friction ball and forms a smooth graphitized surface on the wear track, resulting in long-lasting superlubrication. The strong adhesion between the  $\text{ZrO}_2$  ball,  $\text{Si}_3\text{N}_4$  ball, and SiC ball and the contact interface of a-C:H film causes serious damage to the surface of the friction ball, making the superlubrication fail.

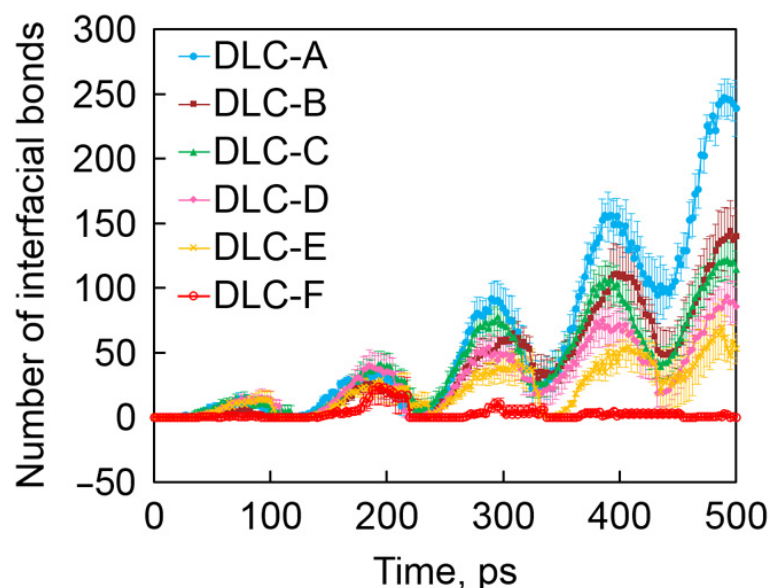


**Figure 5.** Time evolution of the number of interfacial C-C bonds. Rprinted with permission from Ref. [52]. Copyright 2017, WILEY-VCH Verlag GmbH & Co. KGaA, Weinheim.

#### 4.2.2. Effects on Surface Structure

On one hand, one possible change that may occur in an ultra-high vacuum environment is that the dissociative hydrogen ions may dissociate from termination groups on the surface and react with ions or molecules in the surrounding air, thereby affecting the properties of the a-C:H film. On the other hand, in an ultra-high vacuum environment, due to the absence of gases or impurities, the termination groups on the surface of the a-C:H film may undergo rearrangement, altering the structure and properties of the a-C:H film.

## 5. Humid Environment

### 5.1. Nanostructure of Transfer Film

A water vapor environment is a common environment faced by humid areas near the equator, and DLC does not have low friction and wear characteristics in high-humidity environments. Therefore, lubricating oil needs to be added to achieve lubrication in high-humidity environments [73–78]. Therefore, achieving ultra-low friction and reducing the wear of DLC in high-humidity environments is a problem that needs to be solved. By using ceramic-based balls (such as  $\text{Al}_2\text{O}_3$  and  $\text{Si}_3\text{N}_4$  [78]), an altered tip showed a notably low adhesion on the original a-C:H film. It was additionally discovered that the rubbing factor of the a-C:H/ $\text{Al}_2\text{O}_3$  duo steadily declined as the oxygen level on the surface of the a-C:H substrate decreased. This occurrence can be elucidated by a shift in the connective surface from an oxygen ending with potent hydrogen bond connections to a hydrogen ending with feeble van der Waals interactions. By using graphene oxide (GO) nanosheets as additives, the lubrication of silicon-doped DLC (a-C:H: Si) films was achieved, and

the  $\mu$  reached 0.002. On the sliding contact surface of the upper and lower friction pairs, it was found that the surfaces of both were covered by a layer of silicon gel induced by frictional chemistry. At the same time, through the physical adsorption between the upper and lower friction pairs of the friction surface, touched GO nanosheets were transferred from the  $\text{Si}_3\text{N}_4/\text{a-C:H:Si}$  interface to the GO/GO shear interface. This further reduces the shear stress and achieves macroscopic super-slip on a synergistic basis of GO and a-C:H:Si, as shown in Figure 6 [53]. This is similar to the friction of diamonds in humid environments. In high-humidity environments, the  $\mu$  of nanodiamonds is  $\leq 0.05$ , and the wear rate is in the order of  $10^{-10} \text{ mm}^3/(\text{Nm})$ , as shown in Table 1. The passivation mechanism of dangling bonds on the contact surface depends on the fracture of bonds in the slip process (such as contact stress, sliding rate, and temperature settings). The passivation equilibrium is induced by dissociative adsorption of relative humidity, which is the re-hybridization process of graphitized carbon ( $\text{sp}^3 \rightarrow \text{sp}^2$ ). The structure of the interface transfer film is mainly diamond nanoparticles embedded in the amorphous carbon layer. The collision between nanodiamond particles causes friction and the amorphization of chemically induced carbon in the contact area, and then breaks in the uneven contact point, resulting in nanodiamond particles adhering to the amorphous carbon phase [68,79].

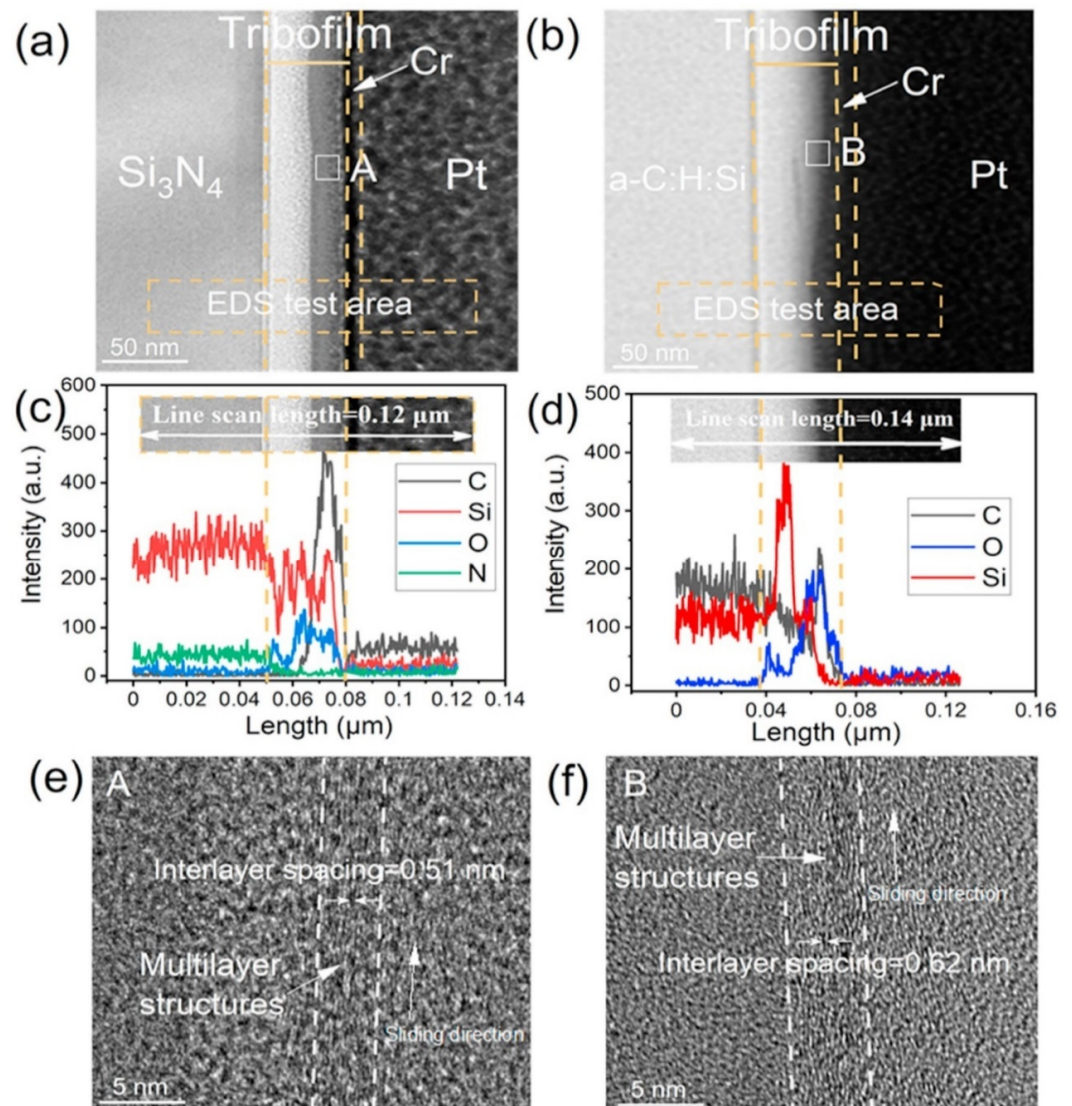


**Figure 6.** The cross-sectional structure of the tribofilm on the  $\text{Si}_3\text{N}_4$  surface and a-C:H:Si film after a friction test. (a,b) The tribofilm formed on the  $\text{Si}_3\text{N}_4$  surface and a-C:H:Si film, respectively.

(c) Elemental distributions along the cross-sectional profile in (a). (d) Elemental distributions along the cross-sectional profile in (b). (e,f) Enlarged views of the tribofilms (area: A and B) formed on the  $\text{Si}_3\text{N}_4$  surface and a-C:H: Si film, respectively. Rprinted with permission from Ref. [53]. Copyright 2017, WILEY-VCH Verlag GmbH & Co. KGaA, Weinheim.

### 5.2. Effects on Surface Structure

In a humid environment, similar to the air environment, there is a high concentration of oxygen, water vapor, and organic compounds, which can cause some physical and chemical changes on the surface of DLC. Firstly, the interaction between water molecules and the hydrogenous surface may result in moisture absorption [80,81], leading to an increase in friction and subsequently an increase in the friction coefficient. Secondly, the positive terminal groups on the surface of a-C:H film are prone to react with water molecules and oxygen in a humid environment, forming hydroxyl groups [82,83]. Unlike the original hydrogenated groups, hydroxyl groups introduce new functional groups, thereby altering the chemical reactivity of the DLC surface and reducing its hydrophobicity. Thirdly, water molecules in a humid environment may form microscopic droplets with passivating groups on the surface [84,85]. These droplets can create an uneven liquid layer on the surface of a-C:H film, increasing the lubrication.

## 6. Lubrication Mechanism

### 6.1. Computational Simulation of the Formation of the Transfer Film

Computational simulation is an emerging research method. With the breakthrough of technology and algorithm innovation, the accuracy of the simulation calculation is increasing, resulting in accurate predictions of the structural properties of materials, avoiding material waste caused by experimental research, and saving costs. For the study of the microstructure and properties of DLC, there are mainly three types of research methods: density functional theory (DFT) simulation based on quantum mechanics, first-principles calculation based on classical mechanics, and MD simulation based on classical mechanics. Some good progress has been made among these methods. MD is a set of molecular simulation methods that mainly rely on Newtonian mechanics to simulate the motion of molecular systems, extract samples from systems composed of different states of molecular systems, and calculate the integral configuration of the system. MD can be used to calculate the thermodynamic properties and other macroscopic properties of the system based on the results of the integral configuration. MD studies atoms or groups of atoms, and the system size is relatively large compared to DFT calculations. The bond length and bond angle between molecules are determined by the force field, making it difficult to carry out detailed research. MD is mostly used for large molecular systems and is often used in conjunction with DFT calculations when studying microproperties, mainly for the construction of DLC models. Through the MD modeling of DLC films, it has been found that the super-slip properties of DLC, that is, surface passivation, mainly depend on two factors [86]: the degree of carbon hybridization and hydrogen content, and the test environment conditions.

For non-hydrogenated DLC, such as a-C or Ta-C films, the molecular modeling design of the friction process simulates interface sliding between graphene-like layers by adjusting the steady-state velocity. This aims to explain the formation of graphitized and carbon-rich transfer layers in the transfer film, as shown in Figure 7 [87–89]. The results show that the formation of well-separated graphene-like interface layers on the interface can be observed when the interlayer spacing is large. The interlayer bond fracture is reduced, and the final bond disappears. That is, triggered by plasticity between adjacent amorphous carbons, the  $\text{sp}^3$  to  $\text{sp}^2$  transition of the carbon phase occurs, greatly increasing the content of  $\text{sp}^2$ -C at the interface and forming a soft amorphous carbon friction transfer layer. Finally, the friction result is super-slip ( $\mu \leq 0.01$ ), that is, a sliding interface with almost no friction and wear. These results are also consistent with the results of super-slip experiments.

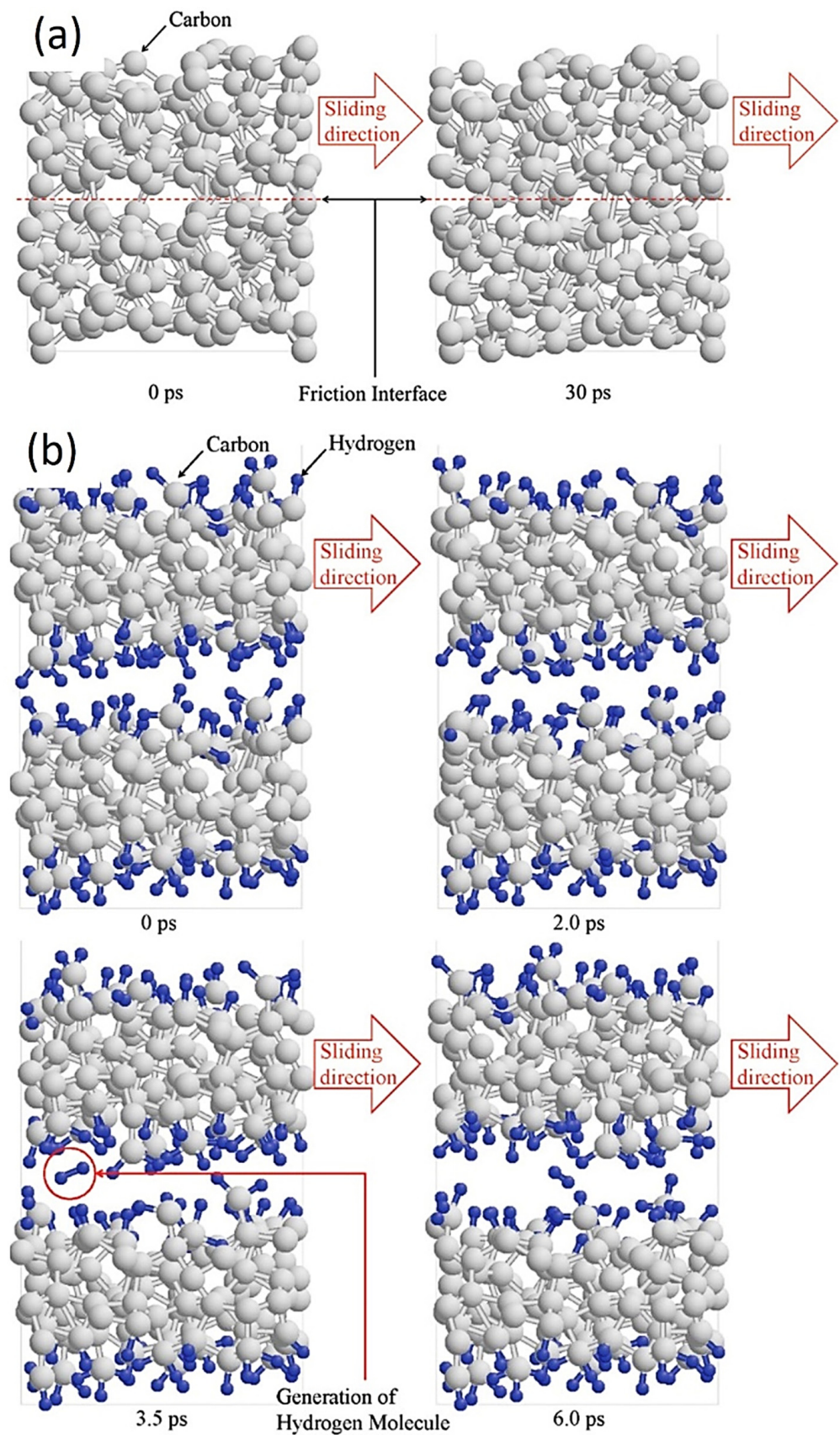


**Figure 7.** Constant height asperity collision simulation of (a) a-C and (b) a-C:H under a load pressure of 1.0 GPa. Rprinted with permission from Ref. [90]. Copyright 2017, WILEY-VCH Verlag GmbH & Co. KGaA, Weinheim.

Compared with non-hydrogenated DLC films, the addition of hydrogen in hydrogenated DLC films leads to a significant reduction in unsaturated carbon bonds at the film interface. These unsaturated carbon atoms serve as contact points for the formation of C-C covalent bonds between the friction pair surface and the a-C:H film [4,90–93]. The adhesive force between these contact points can increase the friction force during sliding. As the sliding time increases, the steric hindrance effect of hydrogen molecules generated can remove the load on the substrate and inhibit the formation of C-C bonds. At the same time, surface hydrogen atoms play a key role in promoting the cleavage of C-C bonds during the sliding process of a-C:H films. As C-C covalent bonds form and break, the number of unsaturated carbon atoms (including  $sp^3$ - and  $sp^2$ -hybridized carbon atoms) decreases, inducing the formation of a transfer film. When covalent bonds break, the friction effect weakens, and the local temperature of the interface increases, leading to the formation of a passivation layer. Compared with DLC films without H or F, a higher  $sp^3$ -C content can cause the DLC film to produce smaller deformation during sliding, thereby reducing the contact area and adhesion [92,93]. In addition, there are a large number of hydrogen or fluorine atoms doped in the DLC film, which form covalent bonds with unsaturated carbon atoms. Non-bonded interactions result in a lower  $\mu$  for a-C:H or a-C:F than for a-C. The anti-bonding effect exists in the friction interface of a-C:F and the repulsive force between the interface atoms is strong. However, a-C:H has weak van der Waals forces on the interface, resulting in a higher  $\mu$  (0.13) for a-C:H than for an a-C:F end DLC model ( $\mu = 0.07$ ). Therefore, the number of unsaturated C-C bonds on the sliding interface is reduced, resulting in a lower adhesive force and a lower steady-state value of interface friction force.

When the tribo-couples are changed, the tribology behavior of a-C:H film changes accordingly, as shown in Figure 8. Mechanical action should also play an important role in the superlubricity of a-C:H films in a vacuum [94–96]. Compared with  $Al_2O_3$ ,  $ZrO_2$ ,  $Si_3N_4$ , and SiC balls have stronger adhesion to the diamond surface. Weak interfacial adhesion contributes to the stable superlubricity of the a-C:H surface (such as the  $Al_2O_3/a-C:H$  interface) under vacuum conditions. However, excessive interfacial adhesion [97–99] can lead to the wear of a-C:H film or the friction pair (such as the  $ZrO_2/a-C:H$ ,  $Si_3N_4/a-C:H$ , and SiC/a-C:H interfaces), both of which shorten the lifespan of superlubricity. The interfacial adhesion between the SiC/a-C:H interfaces is weaker than that of the  $Si_3N_4/a-C:H$  interfaces, but the hardness and contact stress of SiC balls are higher, resulting in more severe wear of the a-C:H film and thus reducing the durability of superlubricity.

By surface doping a-C films with materials such as diamond or methanol, a super-slip model was established, and the simulated friction force was approximately zero [100,101]. Through calculation, it was found that an ultra-thin graphene-like friction layer was formed on the friction interface, and the specific formation reason was shear localization rather than uniform deformation. The main manifestation is the redirection (orientation angle  $< 10^\circ$ ) and phase transition ( $sp^2$ -C ratio  $> 90\%$ ) of C-C covalent bonds that occur preferentially in the friction contact area (graphene-like friction layer) and structural ordering. As the graphene-like sheets gradually aggregate and layer in the friction layer, under the induction of normal stress, the graphene-like sheets transition from adhesive sliding to continuous sliding with ultra-low friction characteristics. This ultimately leads to shear weakening and achieves ultra-low friction. The proposed shear localization mechanism helps to reveal the mechanism of superlubrication.

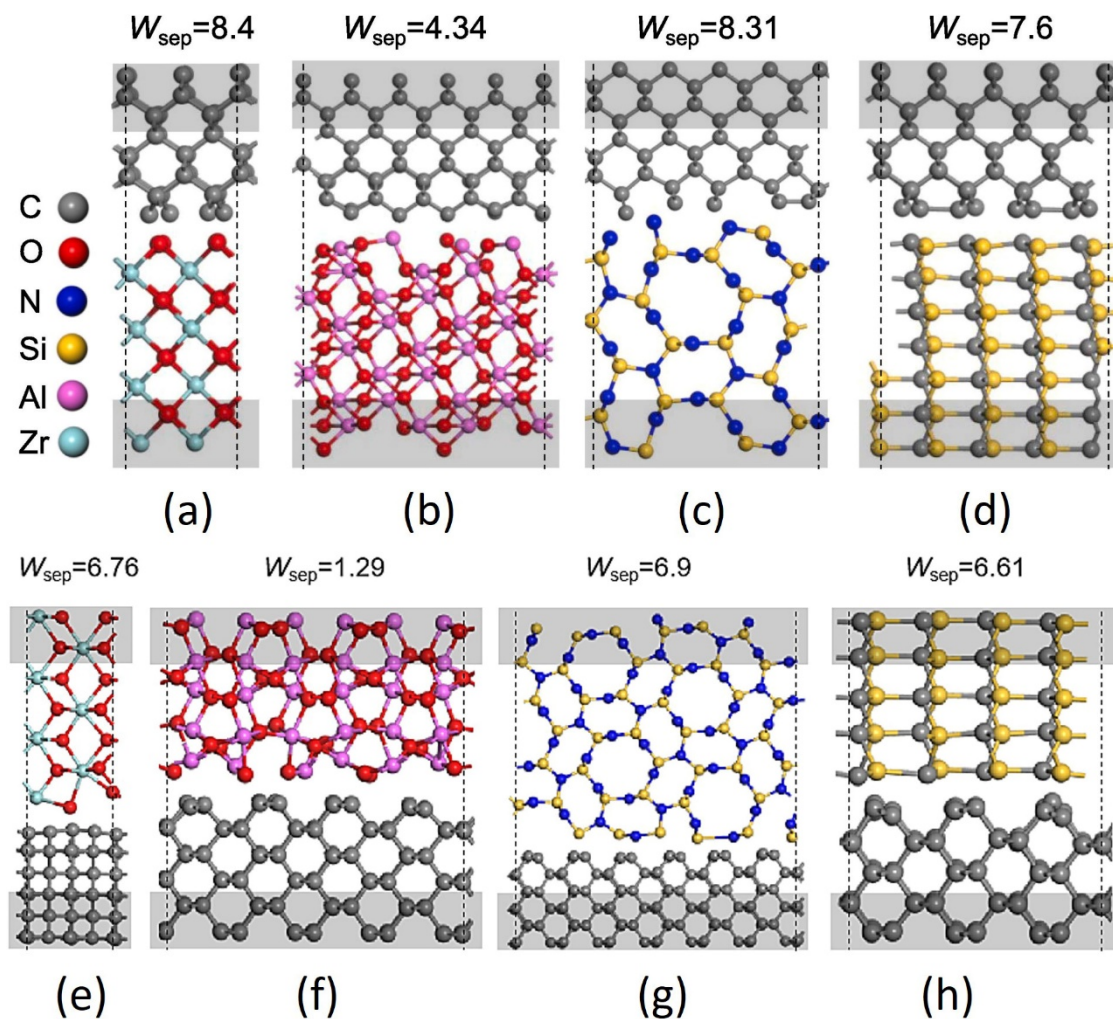


**Figure 8.** Atomic structures: (a)  $ZrO_2(001)/diamond(001)$ , (b)  $Al_2O_3(010)/diamond(001)$ , (c)  $Si_3N_4(110)/diamond(001)$ , (d)  $SiC(110)/diamond(001)$ , (e)  $ZrO_2(101)/diamond(110)$ , (f)  $Al_2O_3(10-2)/diamond(110)$ , (g)  $Si_3N_4(1-30)/diamond(110)$ , (h)  $SiC(1-20)/diamond(110)$ . The calculated works of separation ( $W_{sep}$ ) with  $J/m^2$  in units are marked upon each structure. Rprinted with permission from Ref. [72]. Copyright 2017, WILEY-VCH Verlag GmbH & Co. KGaA, Weinheim.

## 6.2. Material Composition of Tribo-Couples

The appropriate material composition of a-C films plays a crucial role in determining their comprehensive performances. When used as a tribo-couple material, a-C films offer excellent anti-friction and -wear, leading to improved performances and the extended lifespan of a-C films [102,103]. Additionally, their good adhesion to substrates contributes to reduced friction and wear. When selecting counterparts for a mechanical system, one must prioritize their ability to adhere to the substrate, such as metal and ceramic [104–108]. This consideration is vital as it directly impacts on the lubrication properties. The adhesion between the friction pair and the substrate ensures stability and durability, which can avoid slipping or even detachment that would result in system failure. One of the primary factors that affects the tribological performances of a-C film-based counterparts is the film thickness [109–112]. Thicker films are generally associated with higher wear resistance and improved surface hardness to enhance the durability of the frictional system. However, excessive film thickness may lead to increased friction and hinder the smooth sliding motion. Another crucial aspect that affects the tribological performances is the deposition technique (such as plasma-enhanced chemical vapor deposition (PECVD)) used to fabricate the a-C films [40,113–120]. For instance, PECVD films tend to have a higher  $sp^3/sp^2$

carbon ratio, which enhances their hardness and wear resistance. On the other hand, sputtered films exhibit a more amorphous structure, leading to lower friction coefficients. In addition, proper mating materials can help optimize the tribological properties [121–126]. For example, surface materials with low surface roughness can further reduce friction and wear with excellent chemical compatibility. The key to achieving desired tribological performances depends on the suitable thickness of the a-C film, deposition technique, and counterface materials. By considering these factors, researchers can enhance the lubrication performances of a-C film-based systems, enabling their widespread application across various industries.

### 6.3. Comparative Summary of the Formation of the Transfer Film

The formation of an in situ tribofilm is crucial in achieving ultra-wear resistance and low friction coefficients. The structure of the tribofilm plays a key role in its effectiveness, as demonstrated in Figure 9, which summarizes the tribofilms formed under various conditions. These tribofilms exhibit unique formations that enhance their mechanical performance and provide protection against wear and tear. In addition, the presence of certain elements in the environmental conditions or lubricants used can influence the composition and structure of the tribofilms, leading to even greater improvements in wear resistance and friction reduction. Overall, the careful management and optimization of in situ tribofilm formation have the potential to greatly benefit a wide range of industrial applications by providing long-lasting and effective protection against wear and tear.

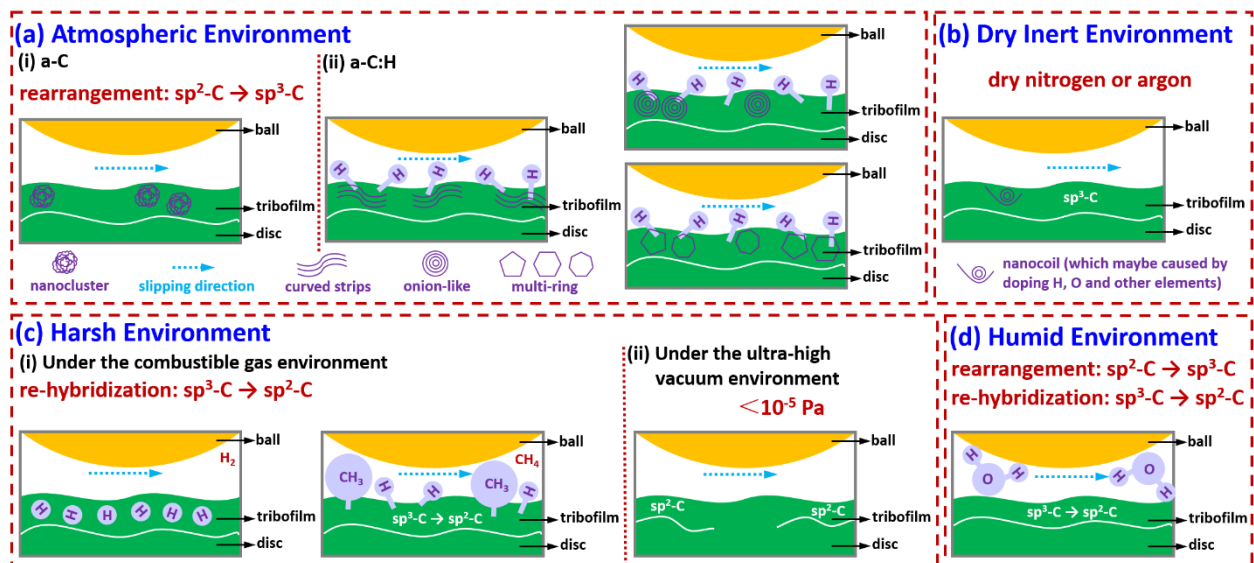


**Figure 9.** Lubrication mechanism diagram of DLC under different service conditions.

#### (a) Atmospheric environment

Under strong shear, unstable  $sp^3$  carbon bonds in a-C break, and their length and direction change, causing adjacent atoms to rearrange along the shear direction to form stable  $sp^2$  carbon bonds and reduce lattice strain energy. Eventually, discontinuous graphite-like nanocrystalline (nanoclusters) transfer materials are formed on the frictional contact surface, and complete graphite-like amorphous carbon is generated along the direction of maximum shear stress. The super-slip mechanism involves the participation of hydrogen atoms, which can weaken the normal electron number of the outermost layer of a-C:H film. Due to lower van der Waals forces, hydrogen end bonds will randomly distribute and cause the outermost electrons to be passivated, further weakening the induced dipole moment and obtaining a lower polarization rate. Finally, a transfer film composed of curved multilayer graphene strips or special structured carbon (such as onion-like or multi-ring) is formed in situ on the frictional sliding contact surface.



(b) Dry inert environment

When non-doped amorphous carbon films that contain elements other than carbon, hydrogen, and oxygen are subjected to friction in a dry nitrogen or argon environment, they create graphitized transfer films on the contact surface, which are rich in  $sp^3$ -C. These transfer films possess chemically inert passivation surfaces, producing macroscopic super-slip effects. However, when the films are doped with other elements, their transfer film structures not only contain graphitized structures but also exhibit new nanostructures due to friction-induced processes. These newly formed structures may exist as nanocoils and can further enhance the friction-reducing properties of the films. Adding these elements greatly enhances the films' super-slip effects, providing optimal conditions for various industrial and mechanical applications.

(c) Harsh environment

(c-i) Under the combustible gas environment

Controlling the target material during the preparation process and controlling the surface or friction chemistry during friction in a hydrogen environment can induce DLC films to form hydrogen-rich transfer materials on the contact surface, achieving a super-slip state. Methane molecules are dissociated into hydrogen and methane groups, which combine with carbon dangling bonds. Through the chemical termination effect of the sliding interface and the re-hybridization process from  $sp^3$ -C to  $sp^2$ -C, the smoothness of the sliding interface is increased, thereby weak interactions are induced between the friction interfaces and low friction and wear are achieved.

(c-ii) Under an ultra-high vacuum environment

Maintaining a suitable level of hydrogen can be advantageous in mitigating methane gas emissions and decreasing atomic-level chemical wear in the transfer film. Additionally, the transfer film structure reveals the presence of graphitized structures, and friction-induced augmentation of the  $sp^2$  bond content in certain locations has a positive effect on the ultra-low friction and wear of hard carbon films.

(d) Humid environment

In increasingly humid environments, the application of DLC can undergo a transformative process, resulting in a combination of surface coatings and DLC that reduces the effects of abrasion and attrition. This unique feature is achieved by these two elements collaborating, working together to form a protective layer on the surface. The interface transfer membrane responsible for this process is created by combining unspecified carbon with graphitized carbon, which undergoes re-hybridization. The result is a layer that is resistant to wear and tear, providing enhanced durability to the material's surface. This attribute is particularly useful in applications where exposure to moisture and other elements can lead to corrosion and degradation, making this type of surface treatment ideal for use in a wide range of settings.

## 7. Conclusions and Perspectives

In the presence of oxygen, the DLC film's surface can oxidize, leading to alterations in its chemical properties and a decline in lubrication performance. However, when in a vacuum or inert gas environments, the DLC film surface experiences a minimal reaction with its surroundings, resulting in outstanding lubrication performance. Alternatively, hydrogen or methane gas can cause gas molecules to dissociate and combine with the carbon dangling bonds on the DLC surface. This process facilitates strong lubrication using chemical termination and graphitization at the sliding interface. Controlling the target material during the preparation process and the surface or friction chemistry during friction in a hydrogen environment can induce a-C:H film to form hydrogen-rich transfer materials on the contact surface, achieving a super-slip state. Methane molecules are dissociated into hydrogen and methane groups, which combine with carbon dangling bonds. Through the chemical termination effect of the sliding interface and the re-hybridization process

from  $sp^3$ -C to  $sp^2$ -C, the smoothness of the sliding interface is increased, thereby weak interactions are induced between the friction interfaces and low friction and wear are achieved. For the tribological properties of a-C films, the composition of the material plays a crucial role. The introduction of elements such as silicon can enhance the hardness and anti-wear properties of a-C films, making them perform well in harsh environments such as high temperatures and high pressure. The introduction of oxygen, fluorine, and other elements can improve the adhesion and corrosion resistance of a-C film and improve its tribological properties in a specific environment. In addition to the addition of elements, the tribological properties of a-C films can also be affected by adjusting the preparation process (such as deposition temperature, deposition rate, and adding metal elements).

Overall, significant advancements have been made with superlubricating a-C film in terms of low friction coefficient and wear resistance. However, several areas require further improvement. Firstly, the preparation technology of superlubricating a-C film needs to be simplified and made more efficient. The current methods, such as PECVD and ion-beam deposition, are complex and costly. Developing simpler and more cost-effective preparation methods would enhance production efficiency and reduce costs. Secondly, the performance stability of superlubricating a-C film needs to be enhanced. While it exhibits excellent wear resistance, its performance may be compromised under harsh conditions like a combustible gas environment. Further research is necessary to improve the stability of the film, ensuring it maintains its excellent performance under various working conditions. Additionally, the application range of superlubricating a-C film should be expanded. Currently, it is primarily utilized in high-end fields like aerospace and electronic equipment. The correspondingly mature products have been applied in high-load-bearing wear-resistant fasteners and self-lubricating bushing in aircrafts. However, applications in other fields are limited in the depositing device and service conditions. Exploring and developing the potential applications of super-slippery carbon film in other industries would broaden its usage and increase its market demand. Although research on the tribofilm of a-C:H film has achieved certain results, there are still some challenges and issues for large-scale utilization. Firstly, enhancing the adhesion of a-C:H films is essential to prevent detachment and ensure their long-term effectiveness. By improving the  $sp^2/sp^3$  ratio or doping of soft metal elements, a-C:H films can offer durable and reliable industrial manufacturing, where friction and wear are prominent concerns. Secondly, the production cost of a-C:H film is high, and the preparation process is complex, which limits the reliability of renewable energy technologies. By combining the coating technique with the deposition technique to enhance the tribological properties, a-C:H film can minimize energy losses and prolong the lifespan of critical parts upon high-load capacity and high wear resistance. Additionally, in the biomedical field, a-C:H film can offer innovative solutions in prosthetics and medical devices. Its low friction characteristics can improve the efficiency and functionality of joint replacements and implants, as it reduces the risk of adverse reactions and enhances patient safety. Overall, with further research, optimization, and cost reduction, a-C:H film holds tremendous potential to revolutionize a wide range of industries in industrial manufacturing, as well as biomedical fields.

**Author Contributions:** The manuscript was written via the contributions of all authors. X.Y. wrote the original draft. Z.J., L.M. and C.L. searched for literature resources. X.Y., H.P. and C.C. confirmed the final draft. H.L., D.L. and B.Z. conceived the conceptualization. All authors have read and agreed to the published version of the manuscript.

**Funding:** This work is supported by the Fundamental Research Funds for the Central Universities (buctrc 202101) and the Tribology Science Fund of the State Key Laboratory of Tribology in Advanced Equipment (SKLTKF23B02).

**Data Availability Statement:** Data available in a publicly accessible repository.

**Conflicts of Interest:** The authors declare no conflicts of interest.

## References

1. Erdemir, U.A.; Eryilmaz, O.L.; Nilufer, I.B.; Fenske, G.R. Synthesis of superlow-friction carbon films from highly hydrogenated methane plasmas. *Surf. Coat. Technol.* **2000**, *133–134*, 448–454. [[CrossRef](#)]
2. Yue, Z.F.; Wang, H.; Fan, X.Q.; Li, H.; Zhang, J.Y.; Zhu, M.H. Regulating the fretting behavior of diamond-like carbon films by changing the composition and structure. *Carbon* **2023**, *212*, 118097. [[CrossRef](#)]
3. Johnson, J.A.; Woodford, J.B.; Erdemir, A.; Fenske, G.R. Near-surface characterization of amorphous carbon films by neutron reflectivity. *Appl. Phys. Lett.* **2003**, *83*, 452–454. [[CrossRef](#)]
4. Stoyanov, P.; Romero, P.A.; Merz, R.; Kopnarski, M.; Stricker, M.; Stemmer, P.; Dienwiebel, M.; Moseler, M. Nanoscale sliding friction phenomena at the interface of diamond-like carbon and tungsten. *Acta Mater.* **2014**, *67*, 395–408. [[CrossRef](#)]
5. Donnet, C. Recent progress on the tribology of doped diamond like and carbon alloy coatings a review. *Surf. Coat. Technol.* **1998**, *100–101*, 180–186. [[CrossRef](#)]
6. Johnson, J.A.; Holland, D.; Woodford, J.B.; Zinovev, A.; Gee, I.A.; Eryilmaz, O.L.; Erdemir, A. Top-surface characterization of a near frictionless carbon film. *Diam. Relat. Mater.* **2007**, *16*, 209–215. [[CrossRef](#)]
7. Chen, X.; Li, J. Superlubricity of carbon nanostructures. *Carbon* **2020**, *158*, 1–23. [[CrossRef](#)]
8. Yu, Q.; Chen, X.; Zhang, C.; Luo, J. Influence Factors on Mechanisms of Superlubricity in DLC Films: A Review. *Front. Mech. Eng.* **2020**, *6*, 65. [[CrossRef](#)]
9. Liu, A.C.Y.; Arenal, R.; Miller, D.J. Structural order in near-frictionless hydrogenated diamondlike carbon films probed at three length scales via transmission electron microscopy. *Phys. Rev. B* **2007**, *75*, 205402. [[CrossRef](#)]
10. Zhang, Z.; Chen, P.; Duan, X.; Zang, K.; Luo, J.; Duan, X. Robust epitaxial growth of two-dimensional heterostructures, multiheterostructures, and superlattices. *Science* **2017**, *357*, 788–792. [[CrossRef](#)]
11. Saravanan, P.; Selyanchyn, R.; Tanaka, H.; Fujikawa, S.; Lyth, S.M.; Sugimura, J. Ultra-low Friction between Polymers and Graphene Oxide Multilayers in Nitrogen Atmosphere, Mediated by Stable Transfer Film Formation. *Carbon* **2017**, *122*, 395–403. [[CrossRef](#)]
12. Eryilmaz, O.L.; Erdemir, A. Surface analytical investigation of nearly-frictionless carbon films after tests in dry and humid nitrogen. *Surf. Coat. Technol.* **2007**, *201*, 7401–7407. [[CrossRef](#)]
13. Heimberg, J.A.; Wahl, K.J.; Singer, I.L.; Erdemir, A. Superlow friction behavior of diamond-like carbon coatings: Time and speed effects. *Appl. Phys. Lett.* **2001**, *78*, 2449–2451. [[CrossRef](#)]
14. Turcheniuk, K.; Trecuzzi, C.; Deelepojananan, C.; Mochalin, V.N. Salt-assisted ultrasonic deaggregation of nanodiamond. *ACS Appl. Mater. Interfaces* **2016**, *8*, 25461–25468. [[CrossRef](#)]
15. Yin, X.; Zhang, J.; Luo, T.; Cao, B.; Xu, J.; Chen, X.; Luo, J. Tribochemical mechanism of superlubricity in graphene quantum dots modified DLC films under high contact pressure. *Carbon* **2021**, *173*, 329–338. [[CrossRef](#)]
16. Yin, X.; Wu, F.; Chen, X.; Xu, J.; Wu, P.; Li, J.; Zhang, C.; Luo, J. Graphene-induced reconstruction of the sliding interface assisting the improved lubricity of various tribo-couples. *Mater. Des.* **2020**, *191*, 108661. [[CrossRef](#)]
17. Berman, D.; Erdemir, A.; Sumant, A.V. Approaches for achieving superlubricity in two-dimensional materials. *ACS Nano* **2018**, *12*, 2122–2137. [[CrossRef](#)] [[PubMed](#)]
18. Chen, X.; Yin, X.; Qi, W.; Zhang, C.; Choi, J.; Wu, S.; Wang, R.; Luo, J. Atomic-scale insights into the interfacial instability of superlubricity in hydrogenated amorphous carbon films. *Sci. Adv.* **2020**, *6*, eaay1272. [[CrossRef](#)] [[PubMed](#)]
19. Chen, X.; Zhang, C.; Kato, T.; Yang, X.; Wu, S.; Wang, R.; Nosaka, M.; Luo, J. Evolution of tribo-induced interfacial nanostructures governing superlubricity in a-C:H and a-C:H:Si films. *Nat. Commun.* **2017**, *8*, 1675. [[CrossRef](#)] [[PubMed](#)]
20. Merkle, A.P.; Erdemir, A.; Eryilmaz, O.L.; Johnson, J.A.; Marks, L.D. In situ TEM studies of tribo-induced bonding modifications in near-frictionless carbon films. *Carbon* **2010**, *48*, 587–591. [[CrossRef](#)]
21. Joly-Pottuz, L.; Matta, C.; de Barros Bouchet, M.I.; Vacher, B.; Martin, J.M.; Sagawa, T. Superlow friction of ta-C lubricated by glycerol: An electron energy loss spectroscopy study. *J. Appl. Phys.* **2007**, *102*, 064912. [[CrossRef](#)]
22. Xu, J.; Luo, T.; Chen, X.; Zhang, C.; Luo, J. Nanostructured tribolayer-dependent lubricity of graphene and modified graphene nanoflakes on sliding steel surfaces in humid air. *Tribol. Int.* **2020**, *145*, 106203. [[CrossRef](#)]
23. Fouts, J.A.; Shiller, P.J.; Mistry, K.K.; Evans, R.D.; Doll, G.L. Additive effects on the tribological performance of WC/a-C:H and TiC/a-C:H coatings in boundary lubrication. *Wear* **2017**, *372–373*, 104–115. [[CrossRef](#)]
24. Benamor, A.; Kota, S.; Chiker, N.; Haddad, A.; Hadji, Y.; Natu, V.; Abdi, S.; Yahi, M.; Benamar, M.E.A.; Sahraoui, T.; et al. Friction and wear properties of MoAlB against Al<sub>2</sub>O<sub>3</sub> and 100Cr6 steel counterparts. *J. Eur. Ceram. Soc.* **2019**, *39*, 868–877. [[CrossRef](#)]
25. Wang, Q.; Zhou, F.; Zhu, L.; Zhang, M.; Kong, J. Mechanical and tribological evaluation of CrSiCN, CrBCN and CrSiBCN coatings. *Tribol. Int.* **2019**, *130*, 146–154. [[CrossRef](#)]
26. Yin, X.; Jin, J.; Chen, X.; Rosenkranz, A.; Luo, J. Ultra-Wear-Resistant MXene-Based Composite Coating via in Situ Formed Nanostructured Tribofilm. *ACS Appl. Mater. Interfaces* **2019**, *11*, 32569–32576. [[CrossRef](#)]
27. Echeverrigaray, F.G.; SR, S.d.M.; Leidens, L.M.; ME, H.M.d.C.; Alvarez, F.; Burgo, T.A.L.; Michels, A.F.; Figueroa, C.A. Towards superlubricity in nanostructured surfaces: The role of van der Waals forces. *Phys. Chem. Chem. Phys.* **2018**, *20*, 21949–21959. [[CrossRef](#)] [[PubMed](#)]
28. Liu, X.; Yang, J.; Hao, J.; Zheng, J.; Gong, Q.; Liu, W. A near-frictionless and extremely elastic hydrogenated amorphous carbon film with self-assembled dual nanostructure. *Adv. Mater.* **2012**, *24*, 4614–4617. [[CrossRef](#)] [[PubMed](#)]

29. Restuccia, P.; Righi, M.C. Tribochemistry of graphene on iron and its possible role in lubrication of steel. *Carbon* **2016**, *106*, 118–124. [[CrossRef](#)]
30. Chen, X.; Yin, X.; Jin, J. A Study on the Wettability of Ion-Implanted Stainless and Bearing Steels. *Metals* **2019**, *9*, 208. [[CrossRef](#)]
31. Wu, P.; Li, X.; Zhang, C.; Chen, X.; Lin, S.; Sun, H.; Lin, C.T.; Zhu, H.; Luo, J. Self-Assembled Graphene Film as Low Friction Solid Lubricant in Macroscale Contact. *ACS Appl. Mater. Interfaces* **2017**, *9*, 21554–21562. [[CrossRef](#)]
32. Murashima, M.; Hojo, K.; Ito, S.; Umehara, N.; Tokoroyama, T.; Takahashi, T.; Imaeda, M. Nanotextured Mold Surface with DLC Coating for Reduction in Residual Ceramic Particles. *Langmuir* **2021**, *37*, 3563–3574. [[CrossRef](#)]
33. Xiang, Z.Y.; Zhang, J.; Xie, S.; Mo, J.; Zhu, S.; Zhai, C. Friction-induced vibration and noise characteristics, and interface tribological behavior during high-speed train braking: The effect of the residual height of the brake pad friction block. *Wear* **2023**, *516*, 204619. [[CrossRef](#)]
34. Zhang, H.B.; Wu, X.H.; Wang, W.Z. Effect of fluid pressure on adhesive wear of spherical contact. *Tribol. Int.* **2023**, *187*, 108723. [[CrossRef](#)]
35. Zhu, X.; Wang, X.; Liu, Y.; Luo, Y.; Liu, Y.; Zhang, H.; Zhao, X. Effect of the Graphitization Mechanism on the Friction and Wear Behavior of DLC Films Based on Molecular Dynamics Simulations. *Langmuir* **2023**, *39*, 1905–1913. [[CrossRef](#)] [[PubMed](#)]
36. Li, Z.; Ma, G.Z.; Xing, Z.G.; Yong, Q.S.; Zhao, H.C.; Huang, Y.F.; Guo, W.L.; Zhang, Z.A.; Wang, H.D. The effects of Cr and B doping on the mechanical properties and tribological behavior of multi-layered hydrogenated diamond-like carbon films. *Surf. Coat. Technol.* **2022**, *431*, 127977. [[CrossRef](#)]
37. Wang, D.-S.; Chang, S.-Y.; Huang, Y.-C.; Wu, J.-B.; Lai, H.-J.; Leu, M.-S. Nanoscopic observations of stress-induced formation of graphitic nanocrystallites at amorphous carbon surfaces. *Carbon* **2014**, *74*, 302–311. [[CrossRef](#)]
38. Cao, Z.; Zhao, W.; Liang, A.; Zhang, J. A General Engineering Applicable Superlubricity: Hydrogenated Amorphous Carbon Film Containing Nano Diamond Particles. *Adv. Mater. Interfaces* **2017**, *4*, 1601224. [[CrossRef](#)]
39. Harada, D.; Tunmee, S.; Euaruksakul, C.; Rittihong, U.; Nakajima, H.; Aono, Y.; Hirata, Y.; Ohtake, N.; Akasaka, H. Investigation of the structure and tribological properties of laser-irradiated hydrogenated amorphous carbon films. *Diam. Relat. Mater.* **2023**, *131*, 109573. [[CrossRef](#)]
40. Xiang, D.; Tan, X.; Sui, X.; He, J.; Chen, C.; Hao, J.; Liao, Z.; Liu, W. Comparative study on microstructure, bio-tribological behavior and cytocompatibility of Cr-doped amorphous carbon films for Co–Cr–Mo artificial lumbar disc. *Tribol. Int.* **2021**, *155*, 106760. [[CrossRef](#)]
41. Gong, Z.; Bai, C.; Qiang, L.; Gao, K.; Zhang, J.; Zhang, B. Onion-like carbon films endow macro-scale superlubricity. *Diam. Relat. Mater.* **2018**, *87*, 172–176. [[CrossRef](#)]
42. Manimunda, P.; Al-Azizi, A.; Kim, S.H.; Chromik, R.R. Shear-Induced Structural Changes and Origin of Ultralow Friction of Hydrogenated Diamond-like Carbon (DLC) in Dry Environment. *ACS Appl. Mater. Interfaces* **2017**, *9*, 16704–16714. [[CrossRef](#)]
43. Wang, Y.; Gao, K.; Zhang, B.; Wang, Q.; Zhang, J. Structure effects of sp<sup>2</sup>-rich carbon films under super-low friction contact. *Carbon* **2018**, *137*, 49–56. [[CrossRef](#)]
44. Wang, J.; Cao, X.; Lu, Z.; Zhang, G.; Xue, Q. The improved mechanical and tribological properties of amorphous carbon film by doping boron carbide. *Ceram. Int.* **2020**, *46*, 9878–9884. [[CrossRef](#)]
45. Zhang, Y.; He, X.; Liu, M.; Zhang, K.; Singh, D.J.; Fan, X.; Wen, M.; Zheng, W. Enabling macroscopic superlubricity in TaC/a-C nanocomposite film by atomic-level Au. *Scr. Mater.* **2023**, *228*, 115329. [[CrossRef](#)]
46. Nosaka, M.; Morisaki, Y.; Fujiwara, T.; Tokai, H.; Kawaguchi, M.; Kato, T. The Run-in Process for Stable Friction Fade-Out and Tribofilm Analyses by SEM and Nano-Indenter. *Tribol. Online* **2017**, *12*, 274–280. [[CrossRef](#)]
47. Erdemir, A.; Eryilmaz, O. Achieving superlubricity in DLC films by controlling bulk, surface, and tribochemistry. *Friction* **2014**, *2*, 140–155. [[CrossRef](#)]
48. Chen, L.; Wu, J.; Lu, Z.; Shang, L.; Zhang, G.; Xue, Q. Probing tribological performances of hydrogenated amorphous carbon film applied in methane by structural modification with boron. *Wear* **2021**, *470–471*, 203610. [[CrossRef](#)]
49. Chen, L.; Wei, X.; Zhang, G.; Shang, L.; Lu, Z.; Nie, X.; Xue, Q. Probing the tribological performances of hydrogenated amorphous carbon film in methane atmosphere based on Hertzian elastic contact model. *Tribol. Int.* **2021**, *155*, 106790. [[CrossRef](#)]
50. Erdemir, A.; Martin, J.M. Superior wear resistance of diamond and DLC coatings. *Curr. Opin. Solid State Mater. Sci.* **2018**, *22*, 243–254. [[CrossRef](#)]
51. Rusanov, A.; Nevshupa, R.; Fontaine, J.; Martin, J.-M.; Le Mogne, T.; Elinson, V.; Lyamin, A.; Roman, E. Probing the tribochemical degradation of hydrogenated amorphous carbon using mechanically stimulated gas emission spectroscopy. *Carbon* **2015**, *81*, 788–799. [[CrossRef](#)]
52. Wang, Y.; Yamada, N.; Xu, J.; Zhang, J.; Chen, Q.; Ootani, Y.; Higuchi, Y.; Ozawa, N.; De Barros Bouchet, M.-I.; Martin, J.M.; et al. Triboemission of hydrocarbon molecules from diamond-like carbon friction interface induces atomic-scale wear. *Sci. Adv.* **2019**, *5*, eaax9301. [[CrossRef](#)] [[PubMed](#)]
53. Yi, S.; Chen, X.; Li, J.; Liu, Y.; Ding, S.; Luo, J. Macroscale superlubricity of Si-doped diamond-like carbon film enabled by graphene oxide as additives. *Carbon* **2021**, *176*, 358–366. [[CrossRef](#)]
54. Yin, X.; Chen, H.; Jiang, L.; Liang, C.; Pang, H.; Liu, D.; Zhang, B. Effects of polyacrylic acid molecular weights on V<sub>2</sub>C-MXene nanocoatings for obtaining ultralow friction and ultralow wear in an ambient working environment. *Phys. Chem. Chem. Phys.* **2022**, *24*, 27406–27412. [[CrossRef](#)] [[PubMed](#)]

55. Khan, A.M.; He, X.; Wu, H.; Desanker, M.; Erdemir, A.; Chung, Y.-W.; Wang, Q.J. Acid Treatment of Diamond-Like Carbon Surfaces for Enhanced Adsorption of Friction Modifiers and Friction Performance. *Tribol. Lett.* **2018**, *66*, 128. [[CrossRef](#)]
56. Kalin, M.; Polajnar, M. The Effect of Wetting and Surface Energy on the Friction and Slip in Oil-Lubricated Contacts. *Tribol. Lett.* **2013**, *52*, 185–194. [[CrossRef](#)]
57. Bellón Vallinot, I.; de la Guerra Ochoa, E.; Echávarri Otero, J.; Chacón Tanarro, E.; Fernández Martínez, I.; Santiago Varela, J.A. Individual and combined effects of introducing DLC coating and textured surfaces in lubricated contacts. *Tribol. Int.* **2020**, *151*, 106440. [[CrossRef](#)]
58. Sun, H.; Yang, L.; Wu, H.; Zhao, L.; Ji, B. Pd nanoparticles lubricant additive catalyze the construction of carbon-based tribofilm to reduce graphitization-induced wear of DLC films under boundary lubrication. *Appl. Surf. Sci.* **2023**, *641*, 158545. [[CrossRef](#)]
59. Ruiz-Lopez, M.F.; Francisco, J.S.; Martins-Costa, M.T.C.; Anglada, J.M. Molecular reactions at aqueous interfaces. *Nat. Rev. Chem.* **2020**, *4*, 459–475. [[CrossRef](#)]
60. Long, Y.; He, P.; Shao, Z.; Li, Z.; Kim, H.; Yao, A.M.; Peng, Y.; Xu, R.; Ahn, C.H.; Lee, S.-W.; et al. Moisture-induced autonomous surface potential oscillations for energy harvesting. *Nat. Commun.* **2021**, *12*, 5287. [[CrossRef](#)]
61. Dangnan, F.; Espejo, C.; Liskiewicz, T.; Gester, M.; Neville, A. Water barrier performance of additively manufactured polymers coated with diamond-like carbon films. *Diam. Relat. Mater.* **2021**, *119*, 108541. [[CrossRef](#)]
62. Ighalo, J.O.; Yap, P.-S.; Iwuozor, K.O.; Aniagor, C.O.; Liu, T.; Dulta, K.; Iwuchukwu, F.U.; Rangabhashiyam, S. Adsorption of persistent organic pollutants (POPs) from the aqueous environment by nano-adsorbents: A review. *Environ. Res.* **2022**, *212*, 113123. [[CrossRef](#)]
63. Awad, A.M.; Jalab, R.; Benamor, A.; Nasser, M.S.; Ba-Abbad, M.M.; El-Naas, M.; Mohammad, A.W. Adsorption of organic pollutants by nanomaterial-based adsorbents: An overview. *J. Mol. Liq.* **2020**, *301*, 112335. [[CrossRef](#)]
64. Topolovec-Miklozic, K.; Lockwood, F.; Spikes, H. Behaviour of boundary lubricating additives on DLC coatings. *Wear* **2008**, *265*, 1893–1901. [[CrossRef](#)]
65. Erdemir, A.; Eryilmaz, O.L.; Nilufer, I.B.; Fenske, G.R. Effect of source gas chemistry on tribological performance of diamond-like carbon films. *Diam. Relat. Mater.* **2000**, *9*, 632–637. [[CrossRef](#)]
66. Erdemir, A.; Eryilmaz, O.L.; Fenske, G. Synthesis of diamondlike carbon films with superlow friction and wear properties. *J. Vac. Sci. Technol. A* **2000**, *18*, 1987–1992. [[CrossRef](#)]
67. Al-Azizi, A.A.; Eryilmaz, O.; Erdemir, A.; Kim, S.H. Surface structure of hydrogenated diamond-like carbon: Origin of run-in behavior prior to superlubricious interfacial shear. *Langmuir* **2015**, *31*, 1711–1721. [[CrossRef](#)]
68. Konicek, A.R.; Grierson, D.S.; Gilbert, P.U.; Sawyer, W.G.; Sumant, A.V.; Carpick, R.W. Origin of ultralow friction and wear in ultrananocrystalline diamond. *Phys. Rev. Lett.* **2008**, *100*, 235502. [[CrossRef](#)] [[PubMed](#)]
69. Zhang, X.; Schneider, R.; Müller, E.; Mee, M.; Meier, S.; Gumbsch, P.; Gerthsen, D. Electron microscopic evidence for a tribologically induced phase transformation as the origin of wear in diamond. *J. Appl. Phys.* **2014**, *115*, 063508. [[CrossRef](#)]
70. Prins, R. Eley–Rideal, the Other Mechanism. *Top. Catal.* **2018**, *61*, 714–721. [[CrossRef](#)]
71. Lin, N.; Lan, H.-Q.; Xu, Y.-G.; Cui, Y.; Barber, G. Coupled Effects between Solid Particles and Gas Velocities on Erosion of Elbows in Natural Gas Pipelines. *Procedia Eng.* **2015**, *102*, 893–903. [[CrossRef](#)]
72. Liu, Y.; Jiang, Y.; Sun, J.; Wang, L.; Liu, Y.; Chen, L.; Zhang, B.; Qian, L. Durable superlubricity of hydrogenated diamond-like carbon film against different friction pairs depending on their interfacial interaction. *Appl. Surf. Sci.* **2021**, *560*, 150023. [[CrossRef](#)]
73. Erdemir, A.; Ramirez, G.; Eryilmaz, O.L.; Narayanan, B.; Liao, Y.; Kamath, G.; Sankaranarayanan, S.K. Carbon-based tribofilms from lubricating oils. *Nature* **2016**, *536*, 67–71. [[CrossRef](#)] [[PubMed](#)]
74. De Barros Bouchet, M.I.; Martin, J.M.; Avila, J.; Kano, M.; Yoshida, K.; Tsuruda, T.; Bai, S.; Higuchi, Y.; Ozawa, N.; Kubo, M.; et al. Diamond-like carbon coating under oleic acid lubrication: Evidence for graphene oxide formation in superlow friction. *Sci. Rep.* **2017**, *7*, 46394. [[CrossRef](#)]
75. Kuwahara, T.; Romero, P.A.; Makowski, S.; Weihnacht, V.; Moras, G.; Moseler, M. Mechano-chemical decomposition of organic friction modifiers with multiple reactive centres induces superlubricity of ta-C. *Nat. Commun.* **2019**, *10*, 151. [[CrossRef](#)]
76. Liu, Y.; Chen, L.; Jiang, B.; Liu, Y.; Zhang, B.; Xiao, C.; Zhang, J.; Qian, L. Origin of low friction in hydrogenated diamond-like carbon films due to graphene nanoscroll formation depending on sliding mode: Unidirection and reciprocation. *Carbon* **2021**, *173*, 696–704. [[CrossRef](#)]
77. Luo, C.; Jiang, Y.; Liu, Y.; Wang, Y.; Sun, J.; Qian, L.; Chen, L. Role of Interfacial Bonding in Tribochemical Wear. *Front. Chem.* **2022**, *10*, 852371. [[CrossRef](#)] [[PubMed](#)]
78. Shi, P.; Sun, J.; Liu, Y.; Zhang, B.; Zhang, J.; Chen, L.; Qian, L. Running-in behavior of a H-DLC/Al<sub>2</sub>O<sub>3</sub> pair at the nanoscale. *Friction* **2020**, *9*, 1464–1473. [[CrossRef](#)]
79. De Barros Bouchet, M.I.; Matta, C.; Vacher, B.; Le-Mogne, T.; Martin, J.M.; von Lantz, J.; Ma, T.; Pastewka, L.; Otschik, J.; Gumbsch, P.; et al. Energy filtering transmission electron microscopy and atomistic simulations of tribo-induced hybridization change of nanocrystalline diamond coating. *Carbon* **2015**, *87*, 317–329. [[CrossRef](#)]
80. Obeisun, O.A.; Finegan, D.P.; Engebretsen, E.; Robinson, J.B.; Taiwo, O.O.; Hinds, G.; Shearing, P.R.; Brett, D.J.L. Ex-situ characterisation of water droplet dynamics on the surface of a fuel cell gas diffusion layer through wettability analysis and thermal characterisation. *Int. J. Hydrog. Energy* **2017**, *42*, 4404–4414. [[CrossRef](#)]
81. Wijshoff, H. Drop dynamics in the inkjet printing process. *Curr. Opin. Colloid Interface Sci.* **2018**, *36*, 20–27. [[CrossRef](#)]

82. Launay, G.; Sadullah, M.S.; McHale, G.; Ledesma-Aguilar, R.; Kusumaatmaja, H.; Wells, G.G. Self-propelled droplet transport on shaped-liquid surfaces. *Sci. Rep.* **2020**, *10*, 14987. [[CrossRef](#)]
83. Villegas, M.; Zhang, Y.; Abu Jarad, N.; Soleymani, L.; Didar, T.F. Liquid-Infused Surfaces: A Review of Theory, Design, and Applications. *ACS Nano* **2019**, *13*, 8517–8536. [[CrossRef](#)] [[PubMed](#)]
84. Ersoy, N.E.; Eslamian, M. Phenomenological study and comparison of droplet impact dynamics on a dry surface, thin liquid film, liquid film and shallow pool. *Exp. Therm. Fluid Sci.* **2020**, *112*, 109977. [[CrossRef](#)]
85. Chen, Z.T.; Nguyen, T.H.; Rumrill, S.M.; Lau, K.K.S. One-Step Bottom-Up Growth of Highly Liquid Repellent Worm-Like Surfaces on Planar Substrates. *Adv. Mater. Interfaces* **2022**, *9*, 2101961. [[CrossRef](#)]
86. Kunze, T.; Gemming, S.; Posselt, M.; Seifert, G. Tribological Aspects of Carbon-Based Nanocoatings—Theory and Simulation. *Z. Für Phys. Chem.* **2011**, *225*, 379–387. [[CrossRef](#)]
87. Ma, T.-B.; Hu, Y.-Z.; Xu, L.; Wang, L.-F.; Wang, H. Shear-induced lamellar ordering and interfacial sliding in amorphous carbon films: A superlow friction regime. *Chem. Phys. Lett.* **2011**, *514*, 325–329. [[CrossRef](#)]
88. Kunze, T.; Posselt, M.; Gemming, S.; Seifert, G.; Konicek, A.R.; Carpick, R.W.; Pastewka, L.; Moseler, M. Wear, Plasticity, and Rehybridization in Tetrahedral Amorphous Carbon. *Tribol. Lett.* **2013**, *53*, 119–126. [[CrossRef](#)]
89. Argibay, N.; Babuska, T.F.; Curry, J.F.; Dugger, M.T.; Lu, P.; Adams, D.P.; Nation, B.L.; Doyle, B.L.; Pham, M.; Pimentel, A.; et al. In-situ tribochemical formation of self-lubricating diamond-like carbon films. *Carbon* **2018**, *138*, 61–68. [[CrossRef](#)]
90. Hayashi, K.; Tezuka, K.; Ozawa, N.; Shimazaki, T.; Adachi, K.; Kubo, M. Tribochemical reaction dynamics simulation of hydrogen on a diamond-like carbon surface based on tight-binding quantum chemical molecular dynamics. *J. Phys. Chem. C* **2011**, *115*, 22981–22986. [[CrossRef](#)]
91. Schall, J.D.; Gao, G.; Harrison, J.A. Effects of Adhesion and Transfer Film Formation on the Tribology of Self-Mated DLC Contacts. *J. Phys. Chem. C* **2010**, *114*, 5321–5330. [[CrossRef](#)]
92. Li, L.; Song, W.; Ovcharenko, A.; Xu, M.; Zhang, G. Effects of atomic structure on the frictional properties of amorphous carbon coatings. *Surf. Coat. Technol.* **2015**, *263*, 8–14. [[CrossRef](#)]
93. Bai, S.; Onodera, T.; Nagumo, R.; Miura, R.; Suzuki, A.; Tsuboi, H.; Hatakeyama, N.; Takaba, H.; Kubo, M.; Miyamoto, A. Friction Reduction Mechanism of Hydrogen- and Fluorine-Terminated Diamond-Like Carbon Films Investigated by Molecular Dynamics and Quantum Chemical Calculation. *J. Phys. Chem. C* **2012**, *116*, 12559–12565. [[CrossRef](#)]
94. Wolloch, M.; Levita, G.; Restuccia, P.; Righi, M.C. Interfacial Charge Density and Its Connection to Adhesion and Frictional Forces. *Phys. Rev. Lett.* **2018**, *121*, 026804. [[CrossRef](#)] [[PubMed](#)]
95. Cui, L.; Lu, Z.; Wang, L. Toward Low Friction in High Vacuum for Hydrogenated Diamondlike Carbon by Tailoring Sliding Interface. *ACS Appl. Mater. Interfaces* **2013**, *5*, 5889–5893. [[CrossRef](#)] [[PubMed](#)]
96. Wu, D.; Ren, S.; Pu, J.; Lu, Z.; Zhang, G.; Wang, L. A comparative study of tribological characteristics of hydrogenated DLC film sliding against ceramic mating materials for helium applications. *Appl. Surf. Sci.* **2018**, *441*, 884–894. [[CrossRef](#)]
97. Liu, Y.; Yu, B.; Cao, Z.; Shi, P.; Zhou, N.; Zhang, B.; Zhang, J.; Qian, L. Probing superlubricity stability of hydrogenated diamond-like carbon film by varying sliding velocity. *Appl. Surf. Sci.* **2018**, *439*, 976–982. [[CrossRef](#)]
98. Wang, L.; Cui, L.; Lu, Z.; Zhou, H. Understanding the unusual friction behavior of hydrogen-free diamond-like carbon films in oxygen atmosphere by first-principles calculations. *Carbon* **2016**, *100*, 556–563. [[CrossRef](#)]
99. Huu, T.L.; Zaïdi, H.; Paulmier, D. Lubricating properties of diamond-like coating. *Wear* **1995**, *181–183*, 766–770. [[CrossRef](#)]
100. Ma, T.B.; Wang, L.F.; Hu, Y.Z.; Li, X.; Wang, H. A shear localization mechanism for lubricity of amorphous carbon materials. *Sci. Rep.* **2014**, *4*, 3662. [[CrossRef](#)]
101. Hayashi, K.; Sato, S.; Bai, S.; Higuchi, Y.; Ozawa, N.; Shimazaki, T.; Adachi, K.; Martin, J.-M.; Kubo, M. Fate of methanol molecule sandwiched between hydrogen-terminated diamond-like carbon films by tribochemical reactions: Tight-binding quantum chemical molecular dynamics study. *Faraday Discuss.* **2012**, *156*, 137–146. [[CrossRef](#)] [[PubMed](#)]
102. Hirayama, T.; Eguchi, Y.; Saeki, K.; Matsuoka, T.; Kikegawa, T. Structural analysis of a-C:H and a-C:H:Si films under high-pressure and high-temperature by synchrotron X-ray diffraction. *Diam. Relat. Mater.* **2016**, *70*, 83–90. [[CrossRef](#)]
103. Liu, X.; Zhang, H.; Liu, C.; Zhang, L.; Wang, Q.; Hu, H.; Zheng, J. Influence of bias patterns on the tribological properties of highly hydrogenated PVD a-C:H films. *Surf. Coat. Technol.* **2022**, *442*, 128234. [[CrossRef](#)]
104. Boeira, C.D.; Cemin, F.; Leidens, L.M.; Weber, J.S.; Michels, A.F.; Aguzzoli, C.; Serra, R.; Evaristo, M.; Fernandes, F.; Alvarez, F.; et al. Adhesion of Amorphous Carbon Nanofilms on Ferrous Alloy Substrates Using a Nanoscale Silicon Interlayer: Implications for Solid-State Lubrication. *ACS Appl. Nano Mater.* **2022**, *5*, 3763–3772. [[CrossRef](#)]
105. Mano, H.; Ohana, T. Evaluation of Anti-Adhesion Characteristics of Diamond-Like Carbon Film by Combining Friction and Wear Test with Step Loading and Weibull Analysis. *Materials* **2021**, *14*, 2746. [[CrossRef](#)]
106. Tillmann, W.; Lopes Dias, N.F.; Stangier, D.; Maus-Friedrichs, W.; Gustus, R.; Thomann, C.A.; Moldenhauer, H.; Debus, J. Improved adhesion of a-C and a-C:H films with a CrC interlayer on 16MnCr5 by HiPIMS-pretreatment. *Surf. Coat. Technol.* **2019**, *375*, 877–887. [[CrossRef](#)]
107. Xu, M.; Cai, X.; Chen, Q.; Kwok, S.C.H.; Chu, P.K. Comparative study of mechanical properties of a-C:H films produced on tungsten pre-implanted stainless steel substrate by plasma immersion ion implantation and deposition. *Diam. Relat. Mater.* **2007**, *16*, 1304–1311. [[CrossRef](#)]

108. Zaharia, T.; Kudlacek, P.; Creatore, M.; Groenen, R.; Persoone, P.; van de Sanden, M.C.M. Improved adhesion and tribological properties of fast-deposited hard graphite-like hydrogenated amorphous carbon films. *Diam. Relat. Mater.* **2011**, *20*, 1266–1272. [[CrossRef](#)]
109. Xie, J.; Komvopoulos, K. Friction, nanostructure, and residual stress of single-layer and multi-layer amorphous carbon films deposited by radio-frequency sputtering. *J. Mater. Res.* **2016**, *31*, 1857–1864. [[CrossRef](#)]
110. Liu, F.-X.; Wang, Z.-L. Thickness dependence of the structure of diamond-like carbon films by Raman spectroscopy. *Surf. Coat. Technol.* **2009**, *203*, 1829–1832. [[CrossRef](#)]
111. Zheng, X.-H.; Wang, T.; Wang, G.-Q.; Zhang, W.-K.; Yang, F.-E. Effects of Mo Single-Layer Thickness on Microstructure and Tribological Behavior of WS<sub>x</sub>/Mo/a-C/Mo Multilayer Films. *Adv. Eng. Mater.* **2021**, *23*, 2001413. [[CrossRef](#)]
112. Hong, C.; Tu, J.; Gu, C.; Zheng, X.; Liu, D.; Li, R.; Mao, S.X. The Effect of Stress Relaxation on the Microstructure and Hardness Evolution of Pure Amorphous-Carbon and C/Ti Multilayer Films. *Adv. Eng. Mater.* **2010**, *12*, 920–925. [[CrossRef](#)]
113. Rashid, N.M.A.; Ritikos, R.; Othman, M.; Khanis, N.H.; Gani, S.M.A.; Muhamad, M.R.; Rahman, S.A. Amorphous silicon carbon films prepared by hybrid plasma enhanced chemical vapor/sputtering deposition system: Effects of r.f. power. *Thin Solid Film.* **2013**, *529*, 459–463. [[CrossRef](#)]
114. Cheng, H.-Y.; Wu, W.-Y.; Ting, J.-M. Microstructure and optical properties of chromium containing amorphous hydrogenated carbon thin films (a-C:H/Cr). *Thin Solid Film.* **2009**, *517*, 4724–4727. [[CrossRef](#)]
115. Awang, R.; Tong, G.B.; Ab. Gani, S.M.; Ritikos, R.; Rahman, S.A. The Effects of Deposition Pressure on the Optical and Structural Properties of d.c. PECVD Hydrogenated Amorphous Carbon Films. *Mater. Sci. Forum* **2006**, *517*, 81–84. [[CrossRef](#)]
116. Anishchik, V.M.; Uglov, V.V.; Kuleshov, A.K.; Filipp, A.R.; Rusalsky, D.P.; Astashynskaya, M.V.; Samtsov, M.P.; Kuznetsova, T.A.; Thiery, F.; Pauleau, Y. Electron field emission and surface morphology of a-C and a-C:H thin films. *Thin Solid Film.* **2005**, *482*, 248–252. [[CrossRef](#)]
117. Sheeja, D.; Tay, B.K.; Sze, J.Y.; Yu, L.J.; Lau, S.P. A comparative study between pure and Al-containing amorphous carbon films prepared by FCVA technique together with high substrate pulse biasing. *Diam. Relat. Mater.* **2003**, *12*, 2032–2036. [[CrossRef](#)]
118. de Moraes, M.A.B.; Durrant, S.F.; Rouxinol, F.P. Electron emission enhanced chemical vapor deposition (EEECVD) for the fabrication of diverse silicon-containing films. *Thin Solid Film.* **2001**, *398–399*, 591–596.
119. Xiao, Y.; Tan, X.; Jiang, L.; Xiao, T.; Xiang, P.; Yan, W. The effect of radio frequency power on the structural and optical properties of a-C:H films prepared by PECVD. *J. Mater. Res.* **2017**, *32*, 1231–1238. [[CrossRef](#)]
120. Turri, R.G.; Santos, R.M.; Rangel, E.C.; da Cruz, N.C.; Bortoleto, J.R.R.; Dias da Silva, J.H.; Antonio, C.A.; Durrant, S.F. Optical, mechanical and surface properties of amorphous carbonaceous thin films obtained by plasma enhanced chemical vapor deposition and plasma immersion ion implantation and deposition. *Appl. Surf. Sci.* **2013**, *280*, 474–481. [[CrossRef](#)]
121. Du, N.; Wei, X.; Li, X.; Chen, Z.; Lu, S.; Ding, J.; Feng, C.; Chen, K.; Qiao, J.; Zhang, D.; et al. Friction reactions induced by selective hydrogenation of textured surface under lubricant conditions. *Friction* **2023**, *12*, 174–184. [[CrossRef](#)]
122. Cui, L.; Bi, C.; Peng, X.; Fan, Y. Probing the role of sp<sup>2</sup>-C in high-temperature tribology of a-C films by a comparative study of ta-C film and a-C film. *Diam. Relat. Mater.* **2023**, *137*, 110127. [[CrossRef](#)]
123. Xiong, W.; Feng, X.; Xiao, Y.; Huang, T.; Li, X.; Huang, Z.; Ye, S.; Li, Y.; Ren, X.; Wang, X.; et al. Fluorine-free prepared two-dimensional molybdenum boride (MBene) as a promising anode for lithium-ion batteries with superior electrochemical performance. *Chem. Eng. J.* **2022**, *446*, 137466. [[CrossRef](#)]
124. Ishikawa, T.; Choi, J. The effect of microstructure on the tribological properties of a-C:H films. *Diam. Relat. Mater.* **2018**, *89*, 94–100. [[CrossRef](#)]
125. Du, N.; Feng, C.; Chen, K.; Qiao, J.; Zhang, D.; Li, X. Friction dependence on the textured structure of an amorphous carbon surface: A reactive molecular dynamics study. *Appl. Surf. Sci.* **2023**, *610*, 155584. [[CrossRef](#)]
126. Chen, X.; Kato, T.; Kawaguchi, M.; Nosaka, M.; Choi, J. Structural and environmental dependence of superlow friction in ion vapour-deposited a-C:H:Si films for solid lubrication application. *J. Phys. D Appl. Phys.* **2013**, *46*, 255304. [[CrossRef](#)]

**Disclaimer/Publisher’s Note:** The statements, opinions and data contained in all publications are solely those of the individual author(s) and contributor(s) and not of MDPI and/or the editor(s). MDPI and/or the editor(s) disclaim responsibility for any injury to people or property resulting from any ideas, methods, instructions or products referred to in the content.